

ปฏิกิริยาไฮโดรจีเนชันแบบเลือกเกิดในวัฏภาคของเหลวของฟีนอลอะเซทีลีนบนอนุภาค
แพลเลเดียมขนาดนาโนบนตัวรองรับมีโซพอร์ซิลิกา



นางสาวนภาพร เทียงชัด


ศูนย์วิทยุทรัพยากร
วิทยานิพนธ์นี้เป็นส่วนหนึ่งของการศึกษาตามหลักสูตรปริญญาวิศวกรรมศาสตรมหาบัณฑิต

สาขาวิชาวิศวกรรมเคมี ภาควิชาวิศวกรรมเคมี
คณะวิศวกรรมศาสตร์ จุฬาลงกรณ์มหาวิทยาลัย

ปีการศึกษา 2552

ลิขสิทธิ์ของจุฬาลงกรณ์มหาวิทยาลัย

LIQUID-PHASE SELECTIVE HYDROGENATION OF PHENYLACETYLENE ON
PALLADIUM NANOPARTICLES SUPPORTED ON MESOPOROUS SILICA



Miss Napaporn Tiengchad

A Thesis Submitted in Partial Fulfillment of the Requirements
for the Degree of Master of Engineering Program in Chemical Engineering

Department of Chemical Engineering

Faculty of Engineering

Chulalongkorn University

Academic Year 2009

Copyright of Chulalongkorn University


Thesis Title LIQUID-PHASE SELECTIVE HYDROGENATION OF
PHENYLACETYLENE ON PALLADIUM NANOPARTICLES
SUPPORTED ON MESOPOROUS SILICA

By Miss Napaporn Tiengchad

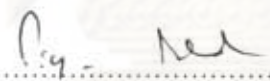
Field of Study Chemical Engineering


Thesis Advisor Assistant Professor Joongjai Panpranot, Ph.D.

Accepted by the Faculty of Engineering, Chulalongkorn University in Partial
Fulfillment of the Requirements for the Master's Degree


..... Dean of the Faculty of Engineering
(Associate Professor Boonsom Lerthirunwong, Dr.Ing.)

THESIS COMMITTEE


..... Chairman
(Professor Piyasan Praserttham, Dr.Ing.)


..... Thesis Advisor
(Assistant Professor Joongjai Panpranot, Ph.D.)


..... Examiner
(Associate Professor Bunjerd Jongsomjit, Ph.D.)


..... External Examiner
(Assistant Professor Okorn Mekasuwandamrong, D.Eng.)

นภาพร เทียงซัด : ปฏิริยาไฮโดรจิเนชันแบบเลือกเกิดในวัฏภาคของเหลวของฟีนิลอะเซทิลีนบนอนุภาคแพลเลเดียมขนาดนาโนบนตัวรองรับมีโซพอร์ซิลิกา. (LIQUID-PHASE SELECTIVE HYDROGENATION OF PHENYLACETYLENE ON PALLADIUM NANOPARTICLES SUPPORTED ON MESOPOROUS SILICA) อ. ที่ปรึกษาวิทยานิพนธ์หลัก : ผศ.ดร.จุงใจ ปั่นประณต, 75 หน้า.

เตรียมตัวเร่งปฏิกิริยาแพลเลเดียมบนมีโซพอร์ซิลิกาที่มีรูพรุนขนาดต่างๆ กัน คือ MCM-41 SBA-15 และ MCF โดยวิธีเคลือบฝัง โดยใช้อนุภาคแขวนลอยของแพลเลเดียมขนาดนาโน และสารละลายแพลเลเดียมอะซิเตท ผลจาก XRD พบว่า MCM-41 และ SBA-15 แสดงลักษณะของโครงสร้างแบบหกเหลี่ยมในขณะที่ MCF แสดงโครงสร้างแบบรังผึ้ง ที่มีขนาดรูพรุน 2.7 3.9 และ 7.8 นาโนเมตร ตามลำดับ อนุภาคแขวนลอยของแพลเลเดียมที่เตรียมขึ้นมีขนาดประมาณ 2.3 นาโนเมตร เมื่อพิจารณาผลจากโครงสร้างรูพรุน พบว่าไม่มีผลต่อขนาดของอนุภาคแพลเลเดียมในตัวเร่งปฏิกิริยา Pd/X_col สำหรับตัวเร่งปฏิกิริยา Pd/X_imp ขนาดของอนุภาคแพลเลเดียมจะเพิ่มขึ้นเมื่อขนาดของรูพรุนเพิ่มขึ้น อย่างไรก็ตาม ตัวเร่งปฏิกิริยา Pd/SBA-15_imp มีขนาดอนุภาคของแพลเลเดียมใหญ่ที่สุดโดยมีรูปร่างเป็นทรงกระบอกเช่นเดียวกับลักษณะของ SBA-15 ตัวเร่งปฏิกิริยา Pd/SBA-15_col เป็นตัวเร่งปฏิกิริยาที่มีประสิทธิภาพมากที่สุดในปฏิกิริยาไฮโดรจิเนชันแบบเลือกเกิดในวัฏภาคของเหลวภายใต้ภาวะที่ไม่รุนแรง (อุณหภูมิ 40 องศาเซลเซียส ความดันของไฮโดรเจน 1 ถึง 5 บาร์ เวลา 30 นาที) โครงสร้างของรูพรุนและขนาดรูพรุนที่เหมาะสมของ SBA-15 ทำให้อนุภาคแพลเลเดียมเข้าไปอยู่ข้างในรูพรุนของ SBA-15 ได้ดี ส่งผลให้มีค่าการเลือกเกิดสไตรีนสูงที่ค่าการเปลี่ยนแปลงของฟีนิลอะเซทิลีนสมบูรณ์ เมื่อทดสอบปฏิกิริยาโดยการนำตัวเร่งปฏิกิริยามาหมุนเวียนใช้ใหม่จำนวน 4 รอบ พบว่าค่าความว่องไวและค่าการเลือกเกิดของตัวเร่งปฏิกิริยา Pd/X_col ไม่เปลี่ยนแปลง ในขณะที่ตัวเร่งปฏิกิริยา Pd/X_imp จะมีค่าความว่องไวที่สูงขึ้นและค่าการเลือกเกิดสไตรีนที่ลดลงในบางกรณี

ภาควิชา.....วิศวกรรมเคมี.....ลายมือชื่อนิสิต.....นภาพร เทียงซัด.....
 สาขาวิชา.....วิศวกรรมเคมี.....ลายมือชื่อ อ.ที่ปรึกษาวิทยานิพนธ์หลัก.....
 ปีการศึกษา.....2552.....

5170579021 : MAJOR CHEMICAL ENGINEERING

KEYWORDS : LIQUID-PHASE SELECTIVE HYDROGENATION / MCM-41 / SBA-15 /
MCF / Pd NANOPARTICLES

NAPAPORN TIENGCHAD : LIQUID-PHASE SELECTIVE HYDROGENATION
OF PHENYLACETYLENE ON PALLADIUM NANOPARTICLES SUPPORTED
ON MESOPOROUS SILICA. THESIS ADVISOR : ASST. PROF. JOONGJAI
PANPRANOT, Ph.D., 75 pp.

A series of palladium catalysts with ca. 1 wt% palladium supported on mesoporous silica with different pore sizes (MCM-41, SBA-15, and MCF) were prepared by deposition of colloidal Pd nanoparticles (Pd/X_col) and Pd(II)acetate solution (Pd/X_imp). MCM-41 and SBA-15 showed the XRD characteristic peaks indicating highly ordered hexagonal pore structure while MCF consisted of spherical cell and frame structure with average pore size of 2.7, 3.9, and 7.8 nm, respectively. Sizes of the colloidal Pd nanoparticles were about 2.3 nm. The supports pore structure did not affect the Pd particle size of Pd/X_col catalysts. For the Pd/X_imp, the Pd particle size was increased with increasing pore diameter of the supports. However, the largest Pd particle size was obtained on Pd/SBA-15_imp since the Pd particles were formed in a long cylindrical shape similar to SBA-15. The Pd/SBA-15_col exhibited the best catalyst performance in the liquid-phase selective hydrogenation of phenylacetylene under mild conditions (40°C, H₂ pressure = 1-5 bar, 30 min). The appropriated pore structure and pore size of SBA-15 could provide a better encapsulation of Pd particles so that high styrene selectivity was attained at complete conversion of phenylacetylene. All the Pd/X_col catalysts exhibited no change in the catalyst activities/selectivity during the recyclability test for four cycles while the Pd/X_imp showed an increase of catalyst activity and lower styrene selectivity in some cases.

Department : ..Chemical Engineering.....

Student's Signature *Napaporn Tiengchad*

Field of Study : ..Chemical Engineering.....

Advisor's Signature *Jan Panpranot*

Academic Year :2009.....

ACKNOWLEDGEMENTS

First of all, the author would like to express my sincere and deepest appreciation to my advisor, Assistant Professor Joongjai Panpranot for her invaluable suggestions, support, encouragement, and help during the course of my graduate study. Without the continuous guidance and comments from Professor Piyasan Prasertdam, this work would never have been achieved. In addition, the author would also be grateful to Professor Piyasan Prasertdam, as the chairman, and Associate Professor Bunjerd Jongsomjit, and Assistant Professor Okorn Makasuwandamrong as the members of the thesis committee.

Most of all, the author would like to express her highest gratitude to her parents who always pay attention to her all the times for their suggestions and have provided support and encouragements. The most success of graduation is devoted to her parents.

Moreover, the author wishes to thank the members of the Center of Excellence on Catalysis and Catalytic Reaction Engineering, Department of Chemical Engineering, Faculty of Engineering, Chulalongkorn University and the member of Chemical Engineering Laboratory for their friendship and assistance. To the many others, not specifically named, who have provided her with support and encouragement, please be assured that she thinks of you.

Finally, the author would like to thank the Thailand Research Fund (TRF), as well as the Graduate School of Chulalongkorn University for their financial supports.

ศูนย์วิจัยทรัพยากร

จุฬาลงกรณ์มหาวิทยาลัย

CONTENTS

	Page
ABSTRACT (THAI).....	iv
ABSTRACT (ENGLISH).....	v
ACKNOWLEDGEMENTS.....	vi
CONTENTS.....	vii
LIST OF TABLES.....	x
LIST OF FIGURES.....	xi
CHAPTER	
I INTRODUCTION.....	1
1.1 Rationale	1
1.2 Objective	3
1.3 Research Scopes	3
1.4 Research Methodology	4
1.5 Research Plan	5
II THEORY.....	6
2.1 Hydrogenation reaction.....	6
2.2 Palladium metal.....	9
2.2.1 Elemental palladium.....	9
2.2.2 Palladium in heterogeneous hydrogenation reactions.....	10
2.3 Mesoporous silicas (MCM-41, SBA-15, and MCF).....	11
III LITERATER REVIEWS.....	17
3.1 Synthesis of Pd nanoparticles.....	17
3.2 Supported Pd catalyst in liquid-phase hydrogenation.....	18
3.3 Role of mesoporous silica in the hydrogenation reaction.....	20
3.4 Comment on the previous works.....	22

	Page
CHAPTER	
IV EXPERIMENTS.....	23
4.1 Catalyst preparations.....	23
4.1.1 Materials.....	23
4.1.2 Preparation of mesoporous silica.....	24
4.1.2.1 MCM-41.....	24
4.1.2.2 SBA-15.....	24
4.1.2.3 MCF.....	25
4.1.3 Preparation of Pd nanoparticles.....	25
4.1.4 Preparation of supported Pd on mesoporous silica.....	26
4.1.4.1 Pd nanoparticles.....	26
4.1.4.2 Pd (II)acetate solution.....	26
4.2 The reaction study in liquid-phase selective hydrogenation.....	27
4.3 Catalysts characterization.....	28
4.3.1 Atomic absorption spectroscopy (AAS).....	28
4.3.2 X-ray diffraction (XRD).....	28
4.3.3 N ₂ physisorption	29
4.3.4 CO-pulse chemisorption.....	29
4.3.5 Transmission electron microscopy (TEM).....	30
4.3.6 X-ray Photoelectron Spectroscopy (XPS).....	30
V RESULTS AND DISCUSSIONS.....	31
5.1 Characterization of the sample before and after reaction.....	31
5.1.1 Mesoporous silica supports characterization.....	31
5.1.1.1 X-Ray Diffraction (XRD).....	31
5.1.1.2 Transmission Electron Microscopy (TEM).....	33
5.1.1.3 N ₂ physisorption.....	34
5.1.2 Pd nanoparticles characterization.....	36
5.1.3 Pd-supported catalysts characterization.....	37

	Page
CHAPTER	
5.1.3.1 X-Ray Diffraction (XRD).....	37
5.1.3.2 Transmission Electron Microscopy (TEM).....	40
5.1.3.3 N ₂ phisorption.....	44
5.1.3.4 CO-Pulse Chemisorption.....	46
5.1.3.5 X-ray Photoelectron Spectroscopy (XPS).....	47
5.2 Catalytic test.....	48
5.3 Characterization of the samples after reaction.....	54
5.3.1 Transmission Electron Microscopy (TEM).....	54
5.3.2 Atomic Absorption Spectroscopy (AAS).....	57
VI CONCLUSIONS AND RECOMMENDATIONS.....	59
6.1 Conclusions.....	59
6.2 Recommendation.....	60
REFERENCES.....	61
APPENDICES.....	66
APPENDIX A CALCULATION FOR CATALYST PREPARATION.....	67
APPENDIX B CALCULATION FOR CO-CHEMISORPTION.....	68
APPENDIX C CHROMATOGRAMS FROM GAS CHROMATOGRAPHY.....	72
APPENDIX D CALCULATION OF PHENYLACTYLENE CONVERSION AND STYRENE SELECTIVITY.....	73
APPENDIX E CALCULATION OF TURNOVER OF FREQUENCY	74
VITA.....	75

LIST OF TABLES

TABLE		Page
2.1	Some physical properties of palladium.....	10
5.1	Pore characteristic of mesoporous silica supports.....	35
5.2	Particle size from TEM analysis.....	44
5.3	Pore characteristic of Pd supported on mesoporous silica.....	45
5.4	CO chemisorptions results of prepared catalysts.....	47
5.5	XPS results of all catalysts.....	48
5.6	Initial reaction results of the catalysts.....	52
5.7	Recyclability of Pd/MCM-41, Pd/SBA-15, and Pd/MCF for four cycles	53
5.8	Actual amount of Pd in the sample before and after reaction for four cycles from AAS technique.....	58



 ศูนย์วิจัยทรัพยากร
 จุฬาลงกรณ์มหาวิทยาลัย

LIST OF FIGURES

FIGURE	Page
2.1	Diagram of hydrogenation reaction..... 7
2.2	Mechanism of hydrogenation of alkyne..... 8
2.3	Path ways of phenylacetylene hydrogenation..... 8
2.4	Variation in the median pore diameter of mesoporous silicas synthesized at different oil-polymer ratios. Pore sizes were determined from N_2 adsorption data using the BdB-FHH method..... 13
2.5	N_2 adsorption-desorption isotherms of mesoporous silicas synthesized at oil-polymer mass ratios of (a) 0.00, (b) 0.21, and (c) 0.50..... 14
2.6	Progression of the morphological transition in P123 templated TEM materials swollen by TMB. The proposed schemes of formation and micrographs of the mesoporous silicas synthesized at oil-polymer mass ratios of (a) 0.00, (b) 0.21, and (c) 0.50 are illustrated..... 15
2.7	SAXS patterns of mesoporous silicas synthesized with oil-polymer mass ratios of (a) 0.00, (b) 0.21, and (c) 0.50..... 16
4.1	The schematic diagram of liquid-phase hydrogenation..... 28
5.1	XRD pattern of mesoporous silica supports..... 32
5.2	TEM image of mesoporous silica supports: MCM-41 observed perpendicular (A) and parallel (B) to the pores; SBA-15 observed perpendicular (C) and parallel (D) to the pores; MCF (E)..... 34
5.3	Pore size distribution of mesoporous silica supports..... 35
5.4	TEM image of Pd nanoparticles in methanol..... 36
5.5	XRD patterns of Pd nanoparticles supported on mesoporous silica..... 38
5.6	XRD pattern of Pd(II)acetate solution supported on mesoporous silica. 38
5.7	XRD pattern of the catalysts in the 2-theta range of $10-80^\circ$ 39

FIGURE	Page
5.8	TEM images of Pd nanoparticles supported on mesoporous silica before test in the hydrogenation reaction..... 43
5.9	Pore size distribution of mesoporous silica before and after Pd loading 46
5.10	Conversion and selectivity of Pd/X_col catalysts in liquid phase selective hydrogenation of phenylacetylene at 40°C, 30 min, H ₂ pressure 1-5 bar..... 49
5.11	Conversion and selectivity of Pd/X_imp catalysts in liquid phase selective hydrogenation of phenylacetylene at 40°C, 30 min, H ₂ pressure 1-5 bar..... 50
5.12	Performance curves of all the catalysts..... 51
5.13	Relation between particle sizes and TOF in the first cycle of selective hydrogenation of phenylacetylene..... 52
5.14	TEM image of catalyst after recycling in selective hydrogenation of phenylacetylene for four cycles..... 57

CHAPTER I

INTRODUCTION

1.1 Rationale

Selective hydrogenation of phenylacetylene is a reaction of industrial importance because phenylacetylene is an unwanted feedstock in the process of styrene production. This compound is a poisoning impurity, causing deactivation of the styrene polymerization catalyst. Thus, phenylacetylene must be removed below 10 ppm in concentration [1-3]. Moreover, selective hydrogenation of phenylacetylene is a very convenient process for catalyst optimization, because it enables both evaluation of process design [4] and quick testing of hydrogenation catalysts [5] under very mild conditions.

In general, the selective hydrogenation reactions are carried out both in gas phase and liquid phase but a large number of these reactions are carried out in liquid-phase using batch type slurry processes. The noble metal or transition metals group VIII are mostly catalyzed in the hydrogenation reactions because they adsorb hydrogen with dissociation and the bonding is not too strong. The major advantages of noble metal catalysts are their relatively high activity, mild process conditions, easy separation, and better handling properties. The noble metals which have an effective in hydrogenation process are Pd, Pt, Rh, and Ru. However, palladium is one of the most frequently used metals in such processes since it has the unique ability to selectively hydrogenation. [6-8]. Moreover, palladium nanoparticles were very promising catalysts in both homogeneous and heterogeneous phase for synthesis of styrene from phenylacetylene under very mild conditions with high selectivity [1-3].

Heterogeneous catalysts are highly significant in many process of industry. Their various advantages include immobilization of the catalytic species on a suitable support, which avoids agglomeration of the active species during chemical reaction, enable easy catalyst recovery, and easy product separation. Therefore, the choice of a suitable support is very important, because the interaction with the active phase may play a critical role in the final performance of the catalysts [3].

Supported Pd catalysts are widely used in liquid-phase hydrogenation for many important organic transformations [9]. The regular supports are use in selective hydrogenation of phenylacetylene composed of carbon [2, 10], SiO₂ [11-114], MCM-41 [12, 14-17], Al₂O₃ [18], TiO₂ [19, 20], zeolite Beta [3]. It is know that a support can affect catalyst activity, selectivity, recycling, refining, material handing, and reproducibility.

Consider to mesoporous silica such as MCM-41, SBA-15, and MCF are of considerable interests. These materials appear especially interesting because their mesoporous may allow an easy access of the large molecules, as that usually involved in the production of fine chemicals, to the active sites [14]. Their main advantages are high BET surface areas, large pore volumes, and highly ordered pore structures with narrow pore size distributions in the range of 2-50 nm, depending on synthesis chemicals and conditions [9, 12].

In this study, the preparation of palladium nanoparticles was studied to enhance activity and selectivity in liquid-phase semihydrogenation of phenylacetylene to styrene under mild condition. The silica materials were used as support such as MCM-41, SBA-15, and MCF. These supports were preparation according to the method reported by Chouyyok W. and coworker [21]. Therefore, this study was focused on the investigation of characteristics and catalytic properties of Pd nanoparticles catalyst supported on mesoporous silica materials.

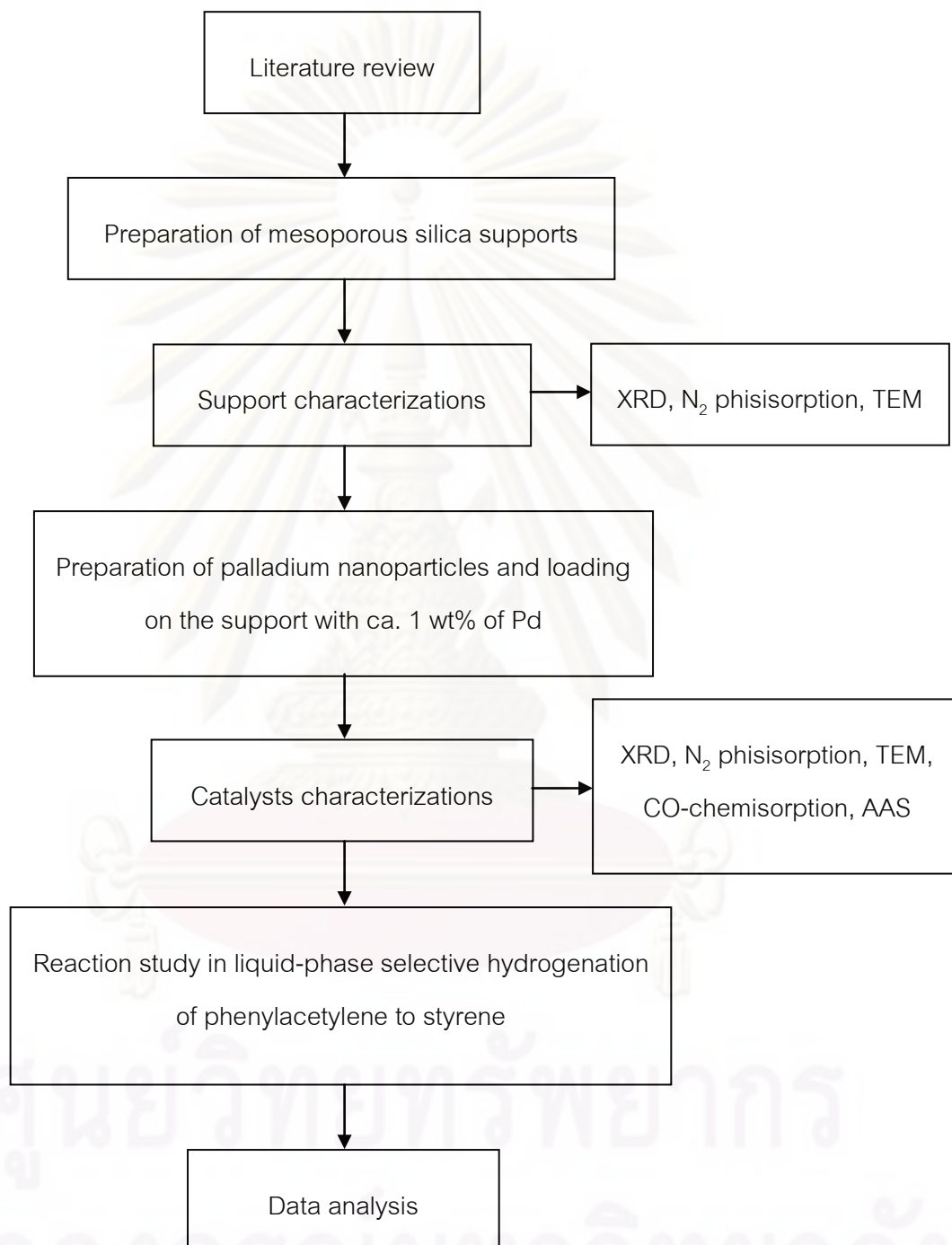
1.2 Objectives

The objective of this research is to investigate the characteristics and catalytic properties of the Pd nanoparticles catalyst supported on mesoporous silicas such as MCM-41, SBA-15, and MCF in the liquid-phase selective hydrogenation of phenylacetylene to styrene.

1.3 Research scopes

1. Synthesis of various mesoporous silica supports as follows;
 - MCM-41
 - SBA-15
 - MCF
2. Synthesis of palladium nanoparticles using reduction by solvent method under an argon atmosphere.
3. Preparation of mesoporous silica supported palladium catalysts using the wet impregnation method with palladium loading of ca. 1 wt %.
4. Characterization of the siliceous-supported palladium catalysts using several techniques, such as atomic absorption spectrometer (AAS), X-ray diffraction (XRD), BET surface area, Transmission electron microscopy (TEM), pulse CO chemisorption.
5. The catalytic performance of the mesoporous silica supported palladium catalysts was studied in the liquid-phase selective hydrogenation of phenylacetylene to styrene using stirring batch reactor (stainless steel autoclave 50 ml).

1.4 Research methodology



1.5 Research plan

Activity	2008				2009												2010			
	9	10	11	12	1	2	3	4	5	6	7	8	9	10	11	12	1	2	3	
Literature Review																				
Mesoporous silica supports preparations																				
Characterization of the supports																				
Pd nanoparticles preparation																				
Catalysts preparations																				
Characterization of the catalysts																				
Reaction study																				
Result analysis																				
Writing a thesis																				

ศูนย์วิทยาศาสตร์
จุฬาลงกรณ์มหาวิทยาลัย

CHAPTER II

THEORY

2.1 Hydrogenation reaction

Catalytic hydrogenation reaction is a well known versatile reaction widely used in organic syntheses. Many functional groups contained in organic substrates can be hydrogenated to produce several useful compounds which has been used for wide applications such as monomers for production of various polymers, fats and oil for producing edible and no edible products, and intermediates used in pharmaceutical industry. Hydrogenation processes are often carried out in a small scale in batch reactor. Batch processes are usually most cost effective since the equipment need not to be dedicated to a single reaction. Typically the catalyst is powdered and slurried with reactant; a solvent is usually present to influence product selectivity and to adsorb the reaction heat liberated by the reaction. Since most hydrogenations are highly exothermic, careful temperature control is required to achieve the desired selectivity and to prevent temperature runaway.

Selective hydrogenation of alkynes is an addition of hydrogen to a carbon-carbon triple bond in order to produce only alkenes product. The overall effect of such an addition is the reductive removal of the triple bond functional group. The simplest source of two hydrogen atoms is molecular hydrogen (H_2), but mixing alkynes with hydrogen does not result in any discernable reaction. However, careful hydrogenation of an alkynes proceeds exclusively to the alkenes until the former is consumed, at which point the product alkenes is very rapidly hydrogenated to an alkanes. Although the overall hydrogenation reaction is exothermic, a high activation energy prevents it from taking place under normal conditions. This restriction may be circumvented by the use of a catalyst, as shown in the following diagram.

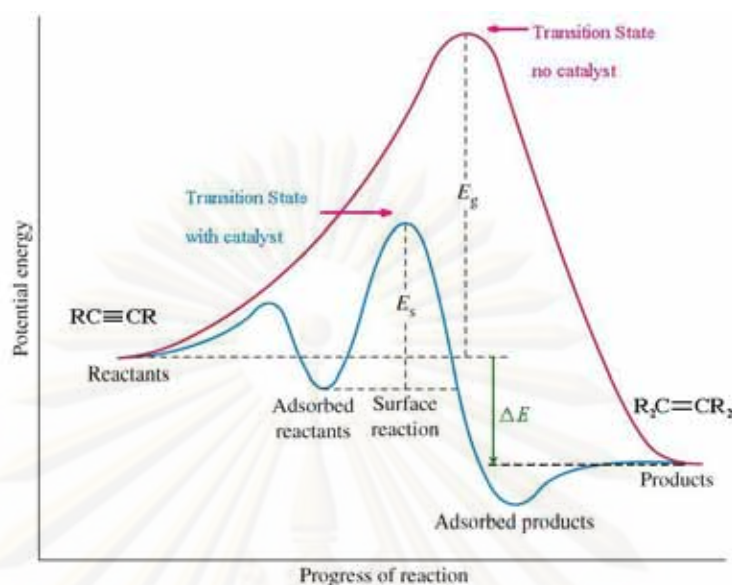


Figure 2.1 Diagram of hydrogenation reaction

Catalysts are substances that change the rate (velocity) of a chemical reaction without being consumed or appearing as part of the product. Catalysts act by lowering the activation energy of reactions, but they do not change the relative potential energy of the reactants and products. Finely divided metals, such as platinum, palladium and nickel, are among the most widely used hydrogenation catalysts.

Selective hydrogenations of alkynes to alkene are the reactions which take place on the surface of the metal catalyst. The mechanism of the reaction can be described in four steps:

Step 1: Hydrogen molecules react with the metal atoms at the catalyst surface. The relatively strong H-H sigma bond is broken and replaced with two weak metal-H bonds.

Step 2: The pi bond of the alkyne interacts with the metal catalyst weakening the bond. A hydrogen atom is transferred from the catalyst surface to one of the carbons of the triple bond.

Step 3: The pi bond of the alkyne interacts with the metal catalyst weakening the bond. A second hydrogen atom is transferred from the catalyst surface forming the alkene.

Step 4: The alkene is released from the catalyst's surface allowing the catalyst to accept additional hydrogen and alkene molecules.

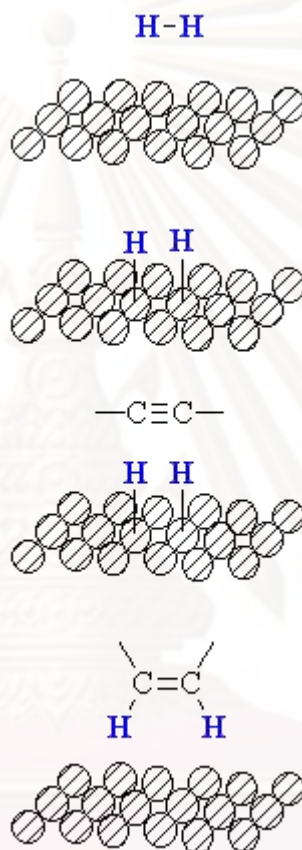


Figure 2.2 Mechanism of hydrogenation of alkyne

Phenyl acetylene hydrogenation scheme consists of two consecutive steps in parallel with a single step directly to the final hydrogenation product.

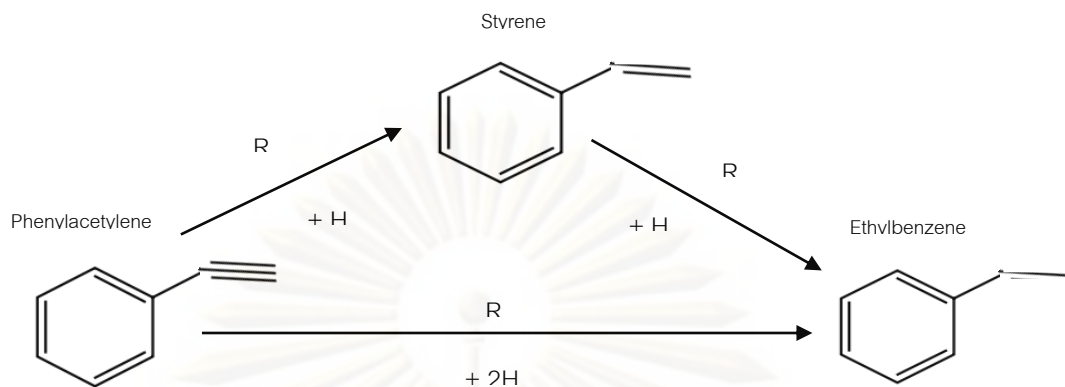


Figure 2.3 Path ways of phenylacetylene hydrogenation

2.2 Palladium metal

2.2.1 Elemental palladium

Palladium as a group VIII noble metal has unique catalytic properties in homogeneous and in heterogeneous reactions. In heterogeneous catalysis palladium is used for oxidation and hydrogenation reactions. One of the most remarkable properties of palladium is the ability to dissociate and dissolve hydrogen. Atomic hydrogen occupies the octahedral interstices between the Pd atoms of the cubic-closed packed metal. Palladium can absorb up to 935 times of its own volume of hydrogen. Depending on hydrogen partial pressure and temperature a so-called α - and β -hydride is formed.

ศูนย์วิทยทรัพยากร

จุฬาลงกรณ์มหาวิทยาลัย

Table 2.1 Some physical properties of palladium.

Atomic number	46
Atomic weight	106.42
Atomic diameter	275.2 pm
Melting point	1827 K
Crystal structure	cubic closed packed
Electron configuration	[Kr] 4d ¹⁰
Electron negativity (Allred & Rochow)	1.4

2.2.2 Palladium in heterogeneous hydrogenation reactions

Like other group VIII metals, palladium can be used for hydrogenation of unsaturated hydrocarbons. Palladium shows the highest selectivity of these metals in heterogeneously catalyzed semi-hydrogenation of alkynes and dienes to the corresponding alkenes. Activity of palladium for hydrocarbon hydrogenation is based on the ability for the dissociative adsorption of hydrogen and chemisorption of unsaturated hydrocarbons. The chemisorption of alkenes and alkynes is based on the interaction of the d-band of the Pd metal with the π -bonding system of the unsaturated hydrocarbons. Industrially used catalysts for acetylene hydrogenation contain relatively low Pd content (< 0.1 wt%) and are supported on metal oxides like alumina. Palladium shows high activity but only limited selectivity and long-term stability for hydrogenation of acetylene. The limited selectivity is mainly due to enhanced ethane formation and the formation of by-products like C₄ and higher hydrocarbons. Palladium shows a strong deactivation behavior because of hydrocarbon and carbon deposits. Catalyst deactivation by hydrocarbon and carbon deposits requires a frequent exchange or regeneration of the catalyst in the hydrogenation reactor. Moreover, fresh or regenerated catalysts show high activity and consequently lead to increased ethylene consumption and reduced

selectivity. Furthermore, high activity of fresh or regenerated catalysts can lead to overheating (“thermal run away”) of the reactor because of the exothermic hydrogenation reaction.

2.3 Mesoporous silicas (MCM-41, SBA-15, and MCF)

Zhao, D., et.al. [22] reported about the mesoporous silica that MCM-41 materials prepared with cationic cetyltrimethylammonium (CTA⁺) surfactants commonly have $d(100)$ spacings of about 40 Å, which after calcination yield a hexagonally ordered porous solid with uniform pore sizes of 20 to 30 Å. Cosolvent organic molecules, such as 1,3,5-trimethylbenzene (TMB) used to expand the pore size of MCM-41 up to 100 Å, unfortunately yield materials with less-resolved x-ray diffraction (XRD) patterns, particularly near the high end of this size range, for which a single broad diffraction peak is often observed. Extended thermal treatment during synthesis gives expanded pore sizes up to ~50Å. We have used post synthesis treatment, by subsequently heating the product obtained from an alkaline S⁺I⁻ synthesis at room temperature in distilled water at pH =7, to obtain pore sizes as large as ;60Å without the need for organic swelling agents. Using CTA1 surfactant species in an L3 sponge phase, McGrath et al. created siliceous solids with large, uniform, but disordered pore assemblies. Pinnavaia and co-workers used nonionic surfactants in neutral aqueous media to synthesize worm-like disordered mesoporous silica with uniform pore sizes of 20 to 58 Å. To increase the dimensions of pore structures produced in such inorganic-organic composite syntheses, we anticipated that the use of amphiphilic polymers of larger molecular weight would extend the mesoscopic-length scales achievable.

Lettow, J. S., et.al. [23] explained the phase transition of hexagonal to mesocellular foam [23] that the lack of stable materials with well-defined pores between the microporous (<20Å) and macroporous (>500Å) regimes was first addressed with the discovery of the M41S materials by Mobil researchers in 1992. However, the pores of the surfactant-templated M41S silicates (20-40 Å) are at the lower end of the

mesoporous regime. The development of SBA-15 silicas and mesostructured cellular foams (MCF) has extended the range of mesoporous materials well past 40 Å. SBA-15 and MCF materials are synthesized with polymer templates and are related by a phase transition from a hexagonally ordered cylindrical mesoporous structure to the mesocellular foam structure.

In the synthesis of MCM-41-type materials, surfactant molecules with small, usually ionic hydrophilic head-groups and hydrophobic alkyl tails are used to template ordered arrays of pores in silica. Diblock and triblock copolymers, with much longer hydrophobic chain lengths than those of surfactants, have been used to template inorganic materials with pore diameters up to ~ 70 Å. In particular, polymer-templated syntheses utilizing a poly(ethylene oxide)-poly(propylene oxide)-poly(ethylene oxide) (PEO-PPO-PEO) triblock copolymer have been successfully developed to create a well-defined mesoporous silica material, termed SBA-15. The use of poly(alkylene oxide) amphiphiles introduces a number of new effects that are important to the phase behavior of these micellar systems and the silica materials they template. First, the hydrophilic group is a long chain rather than a single polar group, so that hydration and entropy effects are very important in determining the shape of the hydrophilic block and the volume that it occupies. The specific nature of PEO and PPO interactions with water is also important. Both PEO and PPO are more soluble in water at low temperatures. PPO is relatively insoluble in water by 20 °C, whereas PEO solutions do not form a second phase until ~ 90 °C.

The differences between ionic surfactant micelles and PEO-PPO-PEO micelles noted above profoundly affect their interactions with hydrophobic "swelling agents". The swelling agents are introduced to supramolecular-templated systems in order to increase the pore size of the inorganic material by preferential solubilization of the additive in the micelle core. 1,3,5-Trimethylbenzene (TMB or mesitylene) has been used previously to swell the pores of surfactant-templated MCM-41 materials. The swelling process maintains the hexagonally packed structure of the cylindrical pores in MCM-41

while increasing pore diameters from 40 to 100 Å. When TMB is added to a PEO-PPO-PEO templated system, the hexagonally packed pore structure is maintained only for very low concentrations of TMB. Upon increasing the oil-polymer ratio, a new mesocellular foam phase is obtained. The MCF phase possesses a system of interconnected pores with diameters of 220-420 Å. In this work, we describe the synthesis conditions of these materials and propose a mechanism for the phase transition of SBA-15 with $p6mm$ symmetry and pore sizes of 40-120 Å to MCF with well-defined pores ranging from 220 to 420 Å in diameter.

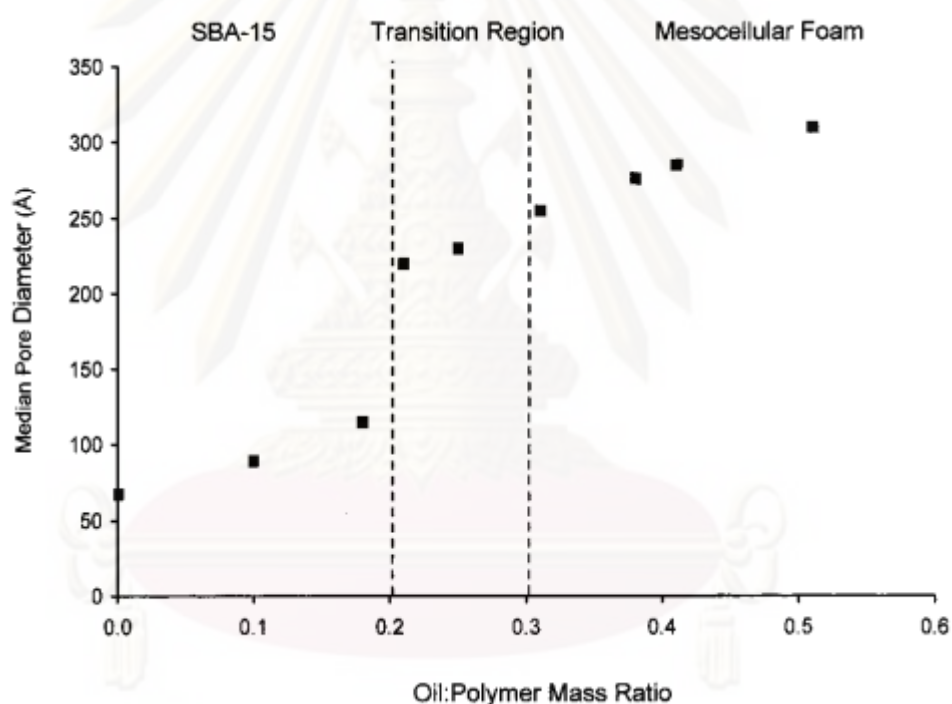


Figure 2.4 Variation in the median pore diameter of mesoporous silicas synthesized at different oil-polymer ratios. Pore sizes were determined from N_2 adsorption data using the BdB-FHH method.

The varying amounts of TMB or “oil”, with the oil-polymer mass ratio ranging from 0 to 0.5 in order to investigate the SBA-15 to mesocellular foam phase transition. A significant increase in the pore size of the mesoporous material is observed at an oil-polymer ratio of ~ 0.2 (see Figure 2.4). The pore diameters reported in Figure 1 were determined by nitrogen adsorption and were verified with TEM. In the low oil

concentration regime, the pores were modeled as long straight cylinders (see Figure 2.5a). For oil-to-polymer ratios above 0.2, the hysteresis in the nitrogen adsorption and desorption isotherms is significantly larger, as shown in Figure 2.5b and c. In the higher oil concentration regime, we used a modification of the Broekhoff-de Boer (BdB) model that treats the pores as spherical cells with smaller openings or windows.

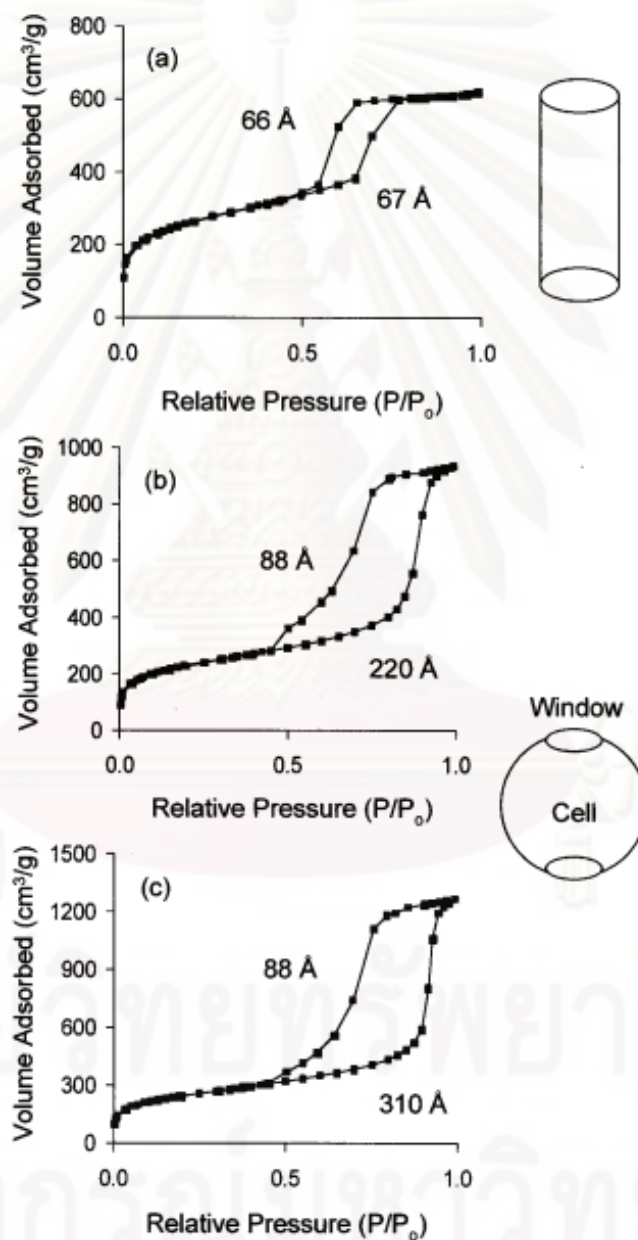


Figure 2.5 N₂ adsorption-desorption isotherms of mesoporous silicas synthesized at oil-polymer mass ratios of (a) 0.00, (b) 0.21, and (c) 0.50.

In addition, the TEM images (Figures 2.6a-c) show a change in pore morphology in the oil-polymer range of 0.2-0.3. The walls of the cylindrical pores begin to buckle with approximately the same periodicity as the pore diameter, forming spherical nodes down the length of the pores as illustrated in Figure 2.6b.

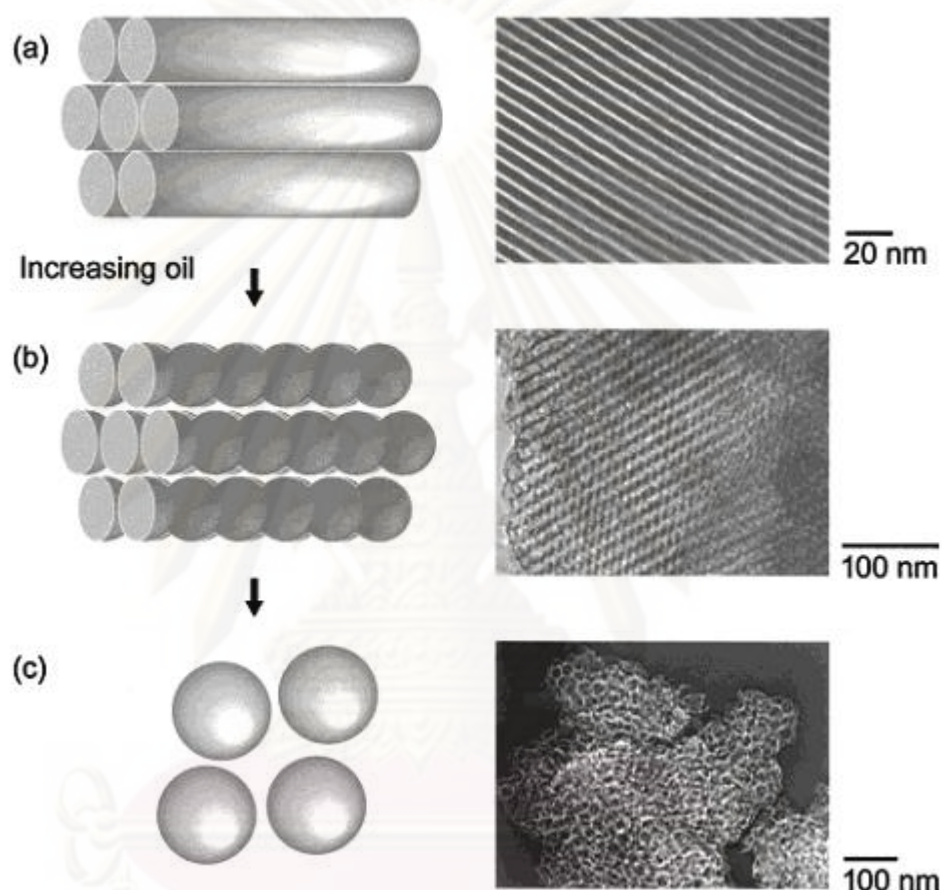


Figure 2.6 Progression of the morphological transition in P123 templated materials swollen by TMB. The proposed schemes of formation and TEM micrographs of the mesoporous silicas synthesized at oil-polymer mass ratios of (a) 0.00, (b) 0.21, and (c) 0.50 are illustrated.

SAXS data indicate a large shift in the d spacing of the primary scattering peak in the transition region of oil-polymer) 0.2-0.3, supporting the TEM and nitrogen adsorption data that also show distinct changes in pore size. However, the SAXS pattern of a sample synthesized with an oil-polymer ratio of 0.21 can still be indexed to the

$p6mm$ space group characteristic of the SBA-15 material (Figure 2.7b). At an oil-polymer ratio of 0.5, the SAXS pattern (Figure 2.7c) does not match the $p6mm$ space group, and can instead be simulated by scattering due to monodisperse spheres characteristic of the mesocellular foam material.

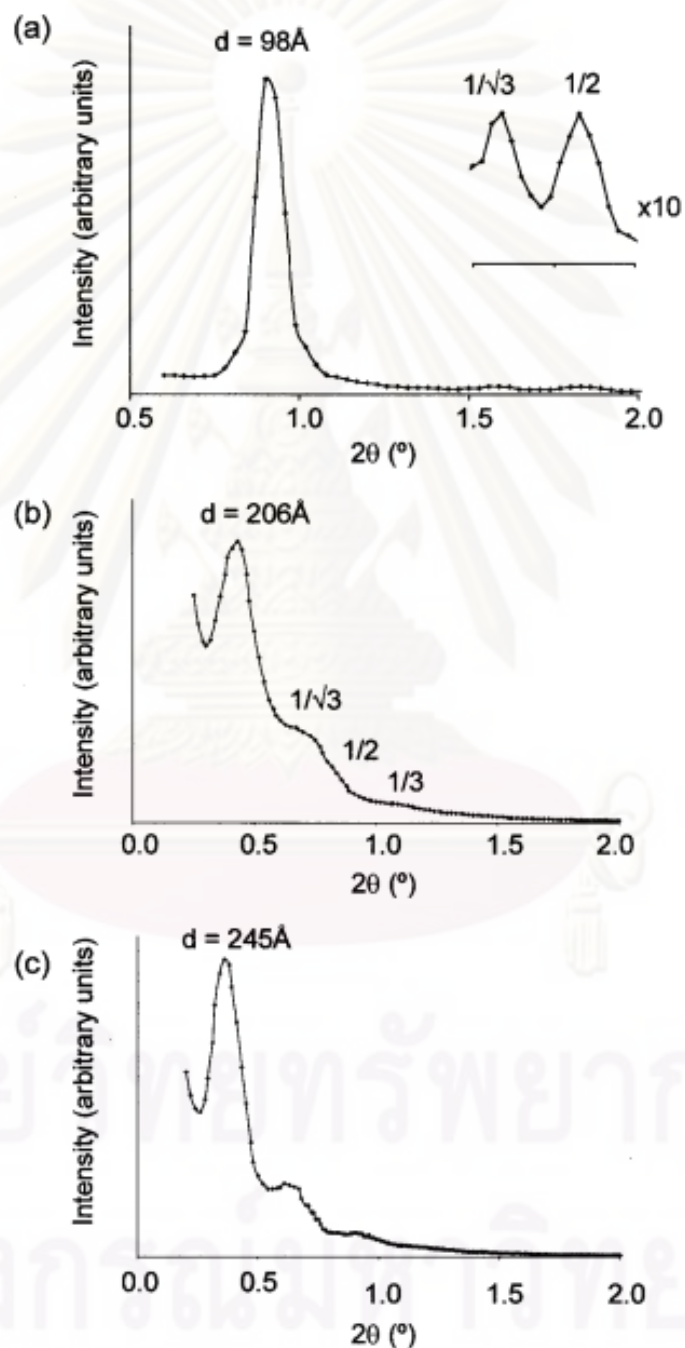


Figure 2.7 SAXS patterns of mesoporous silicas synthesized with oil-polymer mass ratios of (a) 0.00, (b) 0.21, and (c) 0.50.

CHAPTER III

LITERATURE REVIEWS

3.1 Synthesis of palladium nanoparticles

Domínguez-Domínguez, S., *et al.* [1] synthesized the stable mono and bi metallic nanoparticles by using reduction-by-solvent method with different compositions (i.e., Ni-Pd, Fe-Pd, Mg-Pd, Pd, and Pt) and metallic ratios. The average particles size of about 2 nm. All catalysts were tested in liquid-phase semihydrogenation of phenylacetylene to styrene under very mild condition (H_2 pressure = 1 bar and $T = 50^\circ C$). The prepared catalysts show high selectivity toward styrene, while the prepared bimetallic catalysts have proven very active and selective under very mild conditions, showing similar or better results compared with those obtained using pure Pd nanoparticles.

Domínguez-Domínguez, S., *et al.* [2] synthesized Pd colloid using reduction-by-solvent method supported on three types of carbon materials such as multiwall carbon nanotubes (NTs), carbon black (CB), and an activated carbon (AC). All catalysts were tested in liquid-phase semihydrogenation of phenylacetylene to styrene under very mild condition (H_2 pressure = 1 bar and $T = 50^\circ C$). All the Pd/C catalysts exhibited high selectivity toward styrene (>95%) when total conversion was reached. The highest selectivity is obtained for the Pd/NT catalyst, while Pd particle agglomeration find in activated carbon.

Domínguez-Domínguez, S., *et al.* [3] studied the heterogeneous catalyst (palladium nanoparticles) supported on inorganic materials such as γ -alumina, zeolite Beta, MCM-41, and Al-MCM-41 in the liquid-phase semihydrogenation of phenylacetylene under very mild condition. MCM-41 and Al-MCM-41 used the one

alternative method to deposit the Pd nanoparticles called simultaneous synthesis (s.s.). The Pd-supported catalysts exhibited very similar catalytic activity (high selectivity toward styrene as same as previous work). Pd/MCM-41_s.s. and Pd/Al-MCM-41_s.s. show higher TOF of fourfold and sixfold compared with other catalysts related to palladium nanoparticles size and the located of palladium inside the pore.

3.2 Supported Pd catalyst in liquid-phase hydrogenation

David Jackson, S., and Shaw, L.A. [10] studied hydrogenation of phenyl acetylene and styrene over a palladium/carbon catalyst. The kinetics of the reactions were investigated and activation energies of $26 \pm 2 \text{ kJ mol}^{-1}$ $41 \pm 8 \text{ kJ mol}^{-1}$ were obtained for phenyl acetylene hydrogenation and styrene hydrogenation, respectively. Both reactions were found to be zero order concerning the alkyne or alkene. However the order in phenyl acetylene changed from zero order to first order at approximately 60% conversion. This change was due to the effect of styrene co-adsorption and not the concentration of phenyl acetylene. Competitive hydrogenation between the alkene and alkyne resulted in a dramatically reduced rate of hydrogenation for both species. This reduced rate was explained by a reduction in the amount of surface hydrogen as well as the altered bonding of the phenyl acetylene.

Arena, F., *et al.* [24] investigated the catalytic behaviour of palladium supported on oligomeric aramides in the liquid phase selective hydrogenation of phenylacetylene to styrene, by comparison with conventional Pd-supported systems, such as Pd/carbon, Pd/Al₂O₃ and Pd/SiO₂. The influences of the reduction temperature and metal loading on the activity/selectivity of the title reaction are explained in terms of different reducibility patterns of the catalysts, as well as in the light of a peculiar support effect of the organic matrix on Pd particles.

Musolino, M.G., *et al.* [25] studied liquid phase hydrogenation and isomerization of some α,β -unsaturated primary and secondary alcohols have been investigated in tetrahydrofuran over a 2.5% TiO₂ supported palladium catalyst at 303 K and 0.01 MPa partial hydrogen pressure. The double bond isomerization reaction of these substrates leads also to formation of the corresponding saturated aldehydes or ketones. Catalytic activity and selectivity were found to depend strongly on the steric and electronic effects of the substituents on the double bond of the alcohol.

Panpranot, J., *et al.* [26] studied liquid-phase hydrogenation of cyclohexene under mild conditions on Pd/SiO₂ in different organic solvents (benzene, heptanol, and NMP), under pressurized carbon dioxide, and under solvent less condition were investigated and compared. In the cases of using organic solvents, the hydrogenation rates depended on polarity of the solvents in which the reaction rates in high polar solvents such as heptanol and NMP were lower than that in a non-polar solvent. Hydrogenation rates were much higher when the reactions were performed under high-pressure CO₂ or under solvent less condition. The use of high-pressure CO₂ can probably enhance H₂ solubility in the substrate resulting in a higher hydrogenation activity. However, metal sintering and leaching in the presence of high-pressure CO₂ were comparable to those in organic solvents.

Marin-Astorg, N., *et al.* [16] studied the stereoselective hydrogenation of phenyl acetylene and 1-phenyl-1-hexyne at 298 K and atmospheric pressure of H₂ over Pd catalysts supported on mesostructured silica. The catalysts were prepared by the impregnation of HMS and MSU-X silicas with 3-D wormhole framework structures and MCM-41 silica with a 1-D hexagonal framework using a toluene solution of Pd(acac)₂ to obtain a metal content close to 1 wt.%. All the supports were characterised by nitrogen adsorption-desorption isotherms at 77K and XRD. The catalysts were characterized by H₂ chemisorption and TEM measurements. The reactions were found to be zero order with respect to the phenyl acetylene and 1-phenyl-1-hexyne concentration. Each

catalyst presented a different catalytic performance. The 1%Pd/HMS catalyst was the most active in comparison with the 1%Pd/MSU-X and 1%Pd/MCM-41 catalysts. This superior performance in the case of the HMS support was attributed to the presence of interconnected framework channels and textural mesoporosity that can increase the accessibility of the Pd centers to a greater extent than the more monolithic MSU-X and MCM-41 supports. All catalysts displayed high selectivity to styrene and *cis*-1-phenyl-1-hexene compounds.

3.3 Role of mesoporous silica in the hydrogenation reaction.

Panpranot, J., *et al.* [12] studied four types of supported Pd catalysts: Pd/SiO₂ small pore, Pd/SiO₂ large pore, Pd/MCM-41 small pore and Pd/MCM-41 large pore in liquid-phase hydrogenation of 1-hexene. High Pd dispersion was observed on Pd/MCM-41-large pore catalyst while the other catalysts showed relatively low Pd dispersion due to significant amount of Pd being located out of the pores of the supports. Moreover, Pd/MCM-41 large pore showed highest hydrogenation rate with the lowest amount of metal loss.

Mastalir, A., *et al.* [27] synthesized two Pd/MCM-41 catalysts, for which the Pd particles were generated before and after formation of MCM-41 framework (Pd-A and Pd-B), while the Pd particles were synthesis from the reduction of K₂[PdCl₄]. The location and size distribution of the Pd particles were depending on the preparation procedure. The generated of Pd particles before formation of MCM-41 result in Pd particles located external surface of MCM-41 while another catalyst; Pd particles were located inside the mesopore of MCM-41. However, both procedures not affect the Pd particles size. All catalysts were tested in liquid-phase hydrogenation of alkynes: 1-pentyne, 1-hexyne and 3-hexyne. The catalytic activity of Pd-A significantly higher than Pd-B. For Pd-A, the zero order reaction was observed and the initial rate was maintained as the reaction progressed, indicating that the active centers were rapidly accessible for the reactant

molecules. Pd-B show high initial rate of H₂ consumption declined rapidly after a few minutes cause the effect of mass transport limitations, as relate to the encapsulation of Pd particles in MCM-41 structure. Such particles can only be accessed by diffusion of the reactant molecules inside the mesopores, which tends to have a limiting effect on the reaction rate.

Marin-Astorga N. *et al.* [14] studied the liquid-phase hydrogenation of phenyl alkyl acetylenics at 298 K and atmospheric pressure on Pd-supported (siliceous substrates such as amorphous SiO₂, mesoporous MCM-41 and silylated MCM-41) catalysts. A very narrow palladium particle size distribution was observed on the SiO₂ and MCM-41 supports, while the distribution was more heterogeneous on silylated sample. The hydrogenation exhibited a zero order reaction of all catalysts, while the catalytic activity being the most on Pd/MCM-41 catalyst. However, a supported silylated MCM-41 exhibited much lower activity compared with two catalysts whereas a limited access to the channels due to the presence of trimethylsilane groups incorporated in the silylation process, which very voluminous and prevent the entrance of reactants.

Li, H., *et al.* [28] synthesized SBA-15 type mesoporous silica containing surfaces functionalized with aminopropyl and methyl groups (NH₂ and CH₃-SBA-15). After that, the supports were deposition with Ni-B nanoparticles using impregnation method. The TEM results show all of Ni-B/R-SBA-15 samples displayed successive diffraction halos indicative of typical amorphous alloy structure. Ni-B/ NH₂& CH₃-SBA-15 exhibited higher activity and better than either Ni-B/SBA-15 or Ni-B/ NH₂-SBA-15 and Ni-B/ CH₃-SBA-15 in the liquid-phase hydrogenation of *p*-chloronitrobenzene (*p*-CNB) to *p*-chloroaniline (*p*-CAN). Its cause of the aminopropyl incorporated into the silica framework greatly enhanced the dispersion degree of Ni active sites via coordination with Ni²⁺ ions, leading to high hydrogenation activity.

3.4 Comment on the previous works

From the previous studies, Pd is the one of the most useful catalysts used in both homogeneous and heterogeneous phase for hydrogenation reaction. Moreover, the several method for Pd preparation were studied, the one interesting method except impregnation is the synthesized Pd nanoparticles using reduction-by-solvent method to obtain the small Pd particle size. Some of studies use different types of support for comparative Pd nanoparticles in hydrogenation reaction such as γ -alumina, zeolite Beta, MCM-41, Al-MCM-41, and carbon materials. However, no one has studied Pd nanoparticles on the type of mesoporous silica supports even though these materials has high BET surface area, large pore volumes, and highly ordered pore structures with narrow pore size distributions. Thus, the purpose of this study is to investigate the characteristics and catalytic properties of the Pd nanoparticles catalyst supported on mesoporous silicas such as MCM-41, SBA-15, and MCF in liquid-phase selective hydrogenation of phenylacetylene to styrene.

CHAPER IV

EXPERIMENTAL

This chapter describes the experimental procedure used in this research which can be divided into four sections. The preparations of catalysts are shown in section 4.1. The reaction study in phenylacetylene selective hydrogenation is given in section 4.2. Finally, Properties of the catalyst characterized by various techniques are discussed in section 4.3.

4.1 Catalysts preparations

4.1.1 Materials

Chemical	Supplier
Hexadecyltrimethyl-ammonium bromide (CTABr, 99%)	Sigma
Pluronic P123	BASF
Ludox As-40 colloidal silica (40wt.%)	Sigma-Aldrich
Tetraethoxysilane (TEOS, 98%)	Sigma-Aldrich
1,3,5-Trimethylbenzene (TMB)	Supelco
Ammonium solution (NH ₃)	Merck
Acetic acid (CH ₃ COOH)	BDH chemical
Hydrochloric acid (HCl)	J.T. Baker
Silicon dioxide nanopowder 10 nm,99.5%	Aldrich
Silicon dioxide nanopowder 15 nm,99.5%	Aldrich
Ethylene glycol, ≥ 99%	Sigma-Aldrich
Palladium(II)acetate	Sigma-Aldrich
1,4-dioxane	Sigma-Aldrich
Poly(n-vinylpyrrolidone)	Sigma-Aldrich
NaOH	Merck

Chemical	Supplier
Methanol	Merck
Acetone	-
De-ionized water	-

4.1.2 Preparation of mesoporous silica supports

All mesoporous silica supports; consisted of MCM-41, SBA-15, and MCF were synthesized according to the procedure reported by Chouyyok W. *et al.* [21].

4.1.2.1 MCM-41

First solution, 12.15 g CTABr was dissolved in 36.46 g deionized water under vigorous stirring at room temperature to ensure homogenization, then 0.4 g of 25% NH_4OH solution was added and continuing stirred for 30 min. Another solution which composed of 2.66 g NaOH and 20.30 g Ludox in 71.41 g of deionized water was added to the first solution and stirred for another 30 min to obtain homogeneous gel. The gel was poured into a Teflon bottle which closed tightly, and aged at 100°C for 5 days. The pH of gel was adjusted daily by dropwise 30% CH_3COOH solution until the pH became to 10.2. The particles were separated by filtrated and washed with deionized water. Then, dried the particles at 100°C for 16 h, and removed the surfactant template by calcination at 540°C for 6 h.

4.1.2.2 SBA-15

SBA-15 was synthesized by using Pluronic P123 for surfactant template. The solution composed of 4 g Pluronic P123, 30 g of deionized water, and 120 g of HCl (2M). After stirring to ensure the homogenous solution, 8.50 g TEOS was added to the solution and stirred at room temperature for 20 h. A Teflon bottle was used as a

container for kept the solution at 80°C for 24 h. The obtained particles were filtrated and washed with deionized water about ten times. Then, dried at room temperature and calcined at 500°C for 6 h in order to remove the surfactant template.

4.1.2.3 MCF

MCF was preparation by using Pluronic P123 for surfactant template as same as SBA-15. The template (2 g) was dissolved in 75 ml of 1.6M HCl and continuing stirred at 35-40°C until Pluronic P123 was complete dissolved. Afterward, 1g of TMB was added to the solution and stirred to homogeneity. Then, 4.25 g of silica source (TEOS) was added to the mixture and continuing stirred for another 24 h at 35-40°C. Finally, the particles of MCF were filtrated, washed, and done other steps as same as the method for synthesized SBA-15.

4.1.3 Preparation of Pd nanoparticles

The Pd nanoparticles were synthesized by using reduction by solvent method in accordance with the method described by Dominguez S. *et al.* [2]. Ethylene glycol was used to reduce the Pd precursor. The experimental were performed under an Ar atmosphere by mean of a Schlenk system, and the three-necked, round bottom flask were used in the experiment.

Solution A composed of 0.800 g of poly-n-vinyl pyrrolidone and 120 mL of anhydrous ethylene glycol under stirring and heated at 80°C for 3 h. Then, the solution was cooled to 0°C.

Solution B included 0.2245 g of palladium(II)acetate and 50 mL of 1,4-dioxane. The solution was vigorous stirring for 2 h.

Solution B was poured into solution A under stirring and adjusted the pH to 9-10 by dropwise 1 M NaOH solution. The solution was heated at 100 °C under vigorous stirring. After that, the solution was dark brown in color and non transparent, indicating

that the colloid was formed. The heating was continued for 2 h and then, cooled to room temperature.

The prepared Pd nanoparticles colloids were treated with large excess of acetone in order to removed the polymeric protecting agent by centrifugation several times. Finally, the Pd colloid was redispersed in a certain volume of methanol under gentle stirring.

4.1.4 Preparation of supported Pd on mesoporous silica

4.1.4.1 Pd nanoparticles

The Pd nanoparticles were supported on the mesoporous silica using wet impregnation method. First, the appropriate volume of Pd nanoparticles/methanol dispersion was mixed with the mesoporous silica supports. All catalysts were prepared so as to have a final catalyst loading of ca. 1 wt %. The mixture was gentle stirred at room temperature for 3 days and heated at 60 °C for the purpose of removed the methanol solution. The collected solid was washed with 50% ethanol several times. Finally, the catalysts were dried overnight.

4.1.4.2 Pd (II)acetate solution

Pd(II)acetate solution was used as a precursor for preparation the catalysts by incipient wetness impregnation method. The dissolved of necessary content of Pd(II)acetate in acetone was used for this procedure to reached a final loading of ca. 1 wt%. The mesoporous silica supports were impregnated with acetone solution of palladium and kept at room temperature for 6 h. Then, the catalysts were dried at 110°C overnight. At last, the catalysts were calcined in air at 500° for 6 h.

4.2 The Reaction Study in Liquid-Phase Selective Hydrogenation

The liquid-phase selective hydrogenation of phenylacetylene was carried out in two steps. The first step was catalyst preparation and the second step was hydrogenation study.

1. Reduction step

Approximately 0.2 gram of supported Pd catalyst is placed into the autoclave. Then the catalyst is reduced by the hydrogen gas at the volumetric flow rate of 100 ml/min at 40°C for 2 h.

2. Reactant preparation and hydrogenation step

0.5 ml of phenyl acetylene and 4.5 ml of ethanol are mixed in the volumetric flask. Next, the mixture is introduced into the autoclave reactor with 0.005 g of catalyst. Afterward the reactor is filled with hydrogen. The liquid phase hydrogenation is carried out at 40°C for 30 minutes. After the reaction the vent valve is slowly opened to prevent the loss of product. Then the product mixture is analyzed by gas chromatography with flame ionization detector (FID) and the catalyst is characterized by several techniques.

ศูนย์วิจัยทรัพยากร

จุฬาลงกรณ์มหาวิทยาลัย

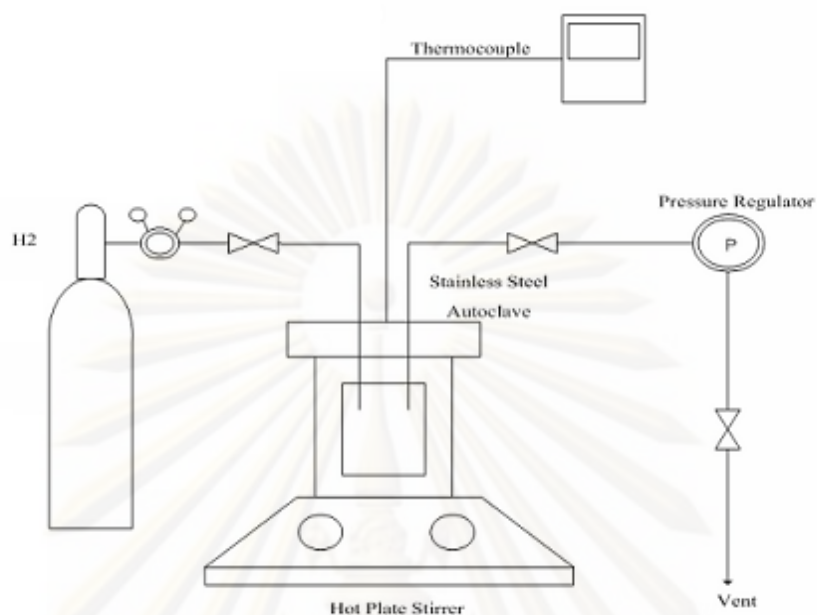


Figure 4.1 The schematic diagram of liquid-phase hydrogenation

4.3 Catalyst Characterization

The properties of the prepared catalyst characterized by various techniques are discussed below.

4.3.1 Atomic Absorption Spectroscopy (AAS)

AAS is a technique for determining the concentration of Pd element in the bulk of catalysts using a Varian Spectra A800 atomic adsorption Spectrometer at the Department of Science Service Ministry of Science and Technology.

4.3.2 X-ray Diffraction (XRD)

The structure of mesoporous silica supports was analyzed using X-ray diffractometer (XRD; Bruker AXS Model D8 Discover), using the Cu K α radiation

($\lambda=0.1542$ nm). The 2θ range scanned was from 0.5° to 6° , with the step size of 0.15 mm.

Otherwise, the bulk crystal structure and chemical phase composition of the prepared catalysts are determined by diffraction of an X-ray beam as a function of the angle of the incident beam. The XRD spectrum of the catalyst is measured by using a SIEMENS D500 X-ray diffractometer and Cu K_α radiation in the 2θ range of 10-80 degree resolution 0.04° . The crystallite size is calculated from Scherrer's equation.

4.3.3 N₂ Physisorption

The adsorption–desorption isotherms were obtained at 77K using a Micromeritics ASAP 2020 automated system. The specific surface area was determined using Brunauer–Emmett–Teller (BET) method. The main pore diameter and pore volume of supports were obtained from the adsorption isotherm branch data and Barret–Joyner–Halenda (BJH) method.

4.3.4 CO-Pulse Chemisorption

The active sites per gram of catalysts and the relative percentages dispersion of palladium catalyst are determined by CO-pulse chemisorption technique using Micromeritics ChemiSorb 2750 (pulse chemisorption system).

Approximately 0.1 g of catalyst was filled in a U-tube, incorporated in a temperature-controlled oven and connected to a thermal conductivity detector (TCD). He was introduced into the reactor at the flow rate of 30 ml/min in order to remove remaining air. Prior to chemisorp, the samples were reduced in a H₂ flow rate at 50 ml/min with heated from room temperature to 40°C and held at this temperature for 2 h. Carbon monoxide that was not adsorbed was measured using thermal conductivity detector. Pulsing was continued until no further carbon monoxide adsorption was observed.

4.3.5 Transmission Electron Microscopy (TEM)

The palladium nanoparticles, mesoporous silica supports, and prepared catalysts are investigated the structure, Pd particles size, and distribution of palladium on silica supported are observed using JEOL-JEM 2010 transmission electron microscope operated at 200 kV.

4.3.6 X-ray Photoelectron Spectroscopy (XPS)

XPS was used to examine the binding energy and the surface composition of the catalysts by using an AMICUS spectrometer with a x-ray source as Mg K_{α} radiation operated at voltage of 20 kV, current of 10 mA. The computer controlled by using the AMICUS "VISION2" software.

CHAPTER V

RESULTS AND DISCUSSION

This chapter presents the results with a discussion about the characteristics and the catalytic properties of mesoporous silica supports; MCM-41, SBA-15, and MCF, including the supported-Pd catalysts in the liquid-phase selective hydrogenation of phenylacetylene to styrene under mild conditions (30 °C, H₂ pressure = 1-5 bar, 30 min). The results and discussions are divided into two sections. The first section described about the characterization of the mesoporous silica supports and the supported-Pd catalyst by using several techniques such as XRD, TEM, N₂-physisorption, CO-chemisorptions, and XPS. The second section reported the catalytic properties of supported-Pd catalysts consisting of the catalysts prepared from Pd nanoparticles using wet impregnation method (Pd/MCM-41_col, Pd/SBA-15_col, and Pd/MCF_col) and the catalysts prepared from Pd(II)acetate using incipient wetness impregnation method (Pd/MCM-41_imp, Pd/SBA-15_imp, and Pd/MCF_imp) in the liquid-phase selective hydrogenation of phenylacetylene.

5.1 Characterization of the samples

5.1.1 Mesoporous silica supports characterization

The mesoporous silica supports were characterized by means of XRD, TEM, N₂ physisorption in order to investigate the structure and morphology.

5.1.1.2 X-Ray Diffraction (XRD)

Pore structure of the mesoporous silica supports are shown in Figure 5.1. The XRD was measured in 2θ range of 0.5-6° for SBA-15 and MCF and 1.5-6° for MCM-41. The XRD pattern of MCM-41 shows the four characteristic Bragg peaks (Reflections 100, 110, 200, 210), indicating a hexagonal pore ordering structure [27, 29- 31], The (100)

plane exhibited highest intensity, while the other peaks showed weaker intensity, which can be taken as an indication of the higher long range ordering of the mesoporous channels. The hexagonal pore structure of SBA-15 was also present from the characteristic XRD pattern in Figure 5.1, corresponding to the reflection (100), (110), and (200) plane [28]. The characteristic pattern confirming a hexagonal order structure was also observed for the last mesoporous silica support (MCF). The shift of characteristic peaks to lower angle of MCF confirmed the larger mesopore size than MCM-41 and SBA-15 [29]. Furthermore, all the mesoporous silica supports did not displayed any diffraction peaks in the 2θ higher than 6° , indicating that the samples are not crystalline at an atomic level [31] (results not shown here).

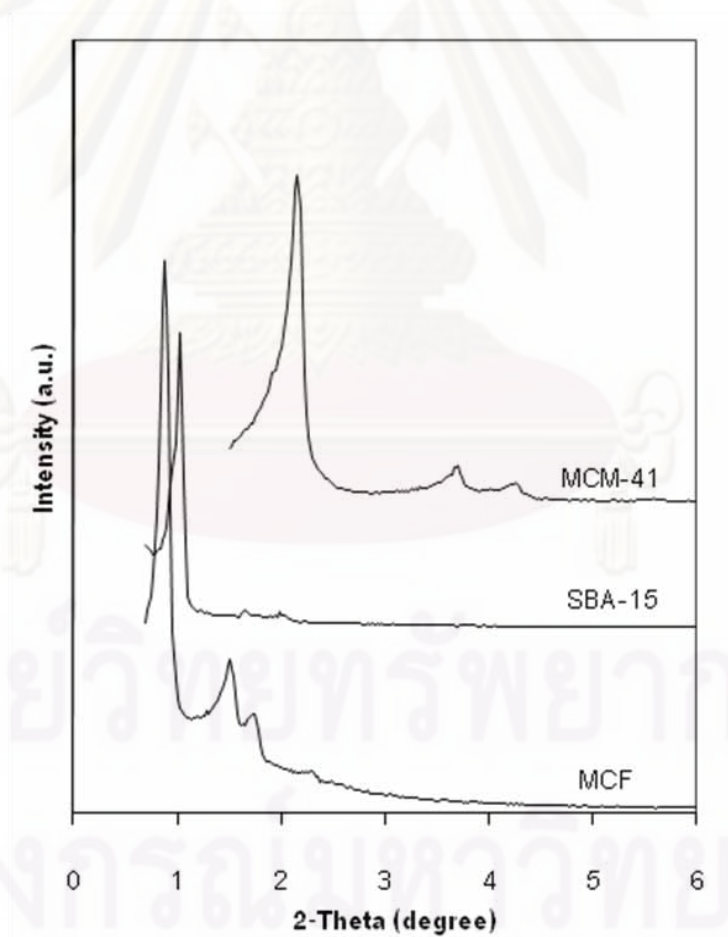
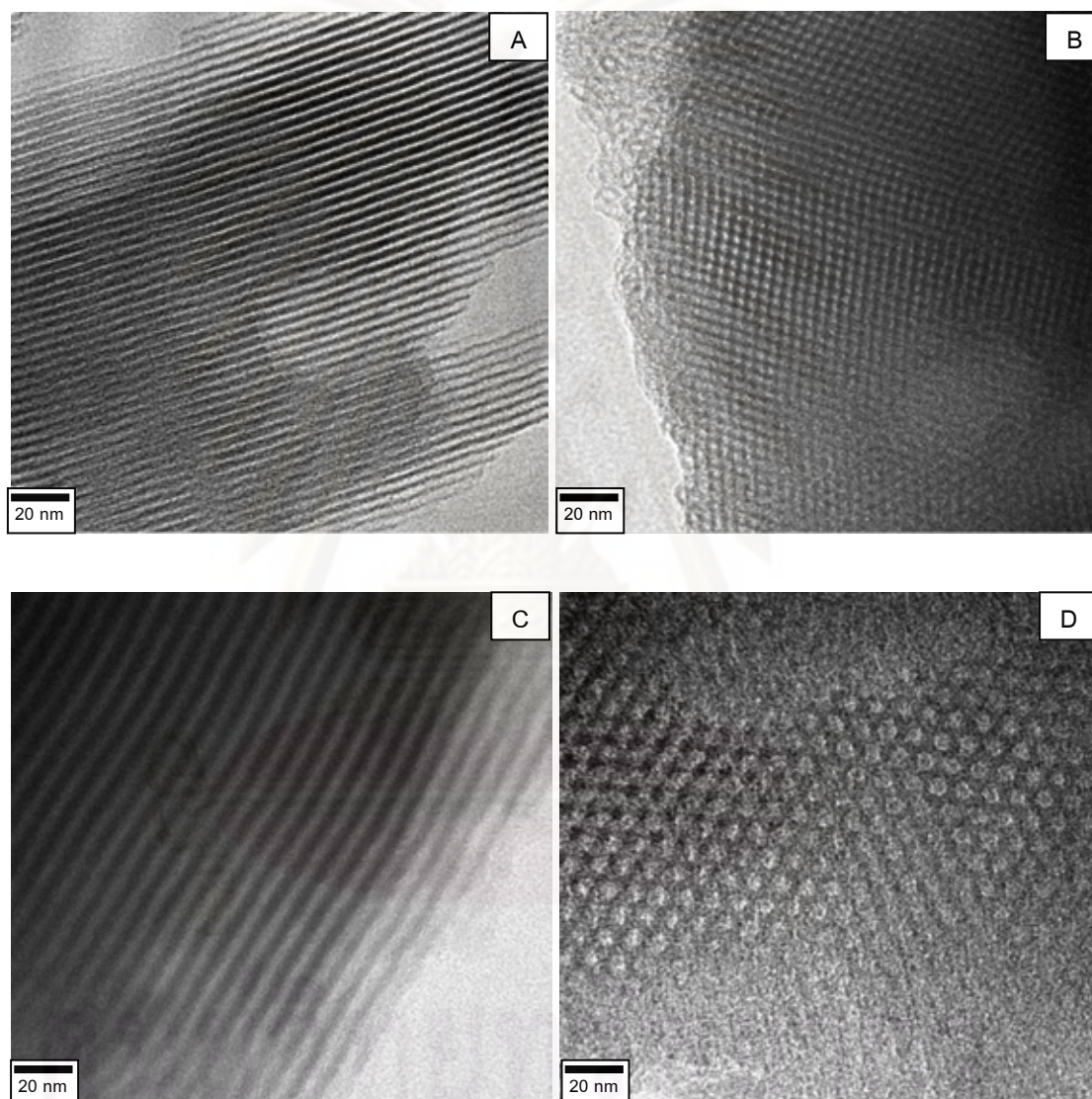


Figure 5.1 XRD pattern of mesoporous silica supports

5.1.1.3 Transmission Electron Microscopy (TEM)

TEM analysis was used to investigate the pore structure, pore size, and morphology of the various mesoporous silica supports.



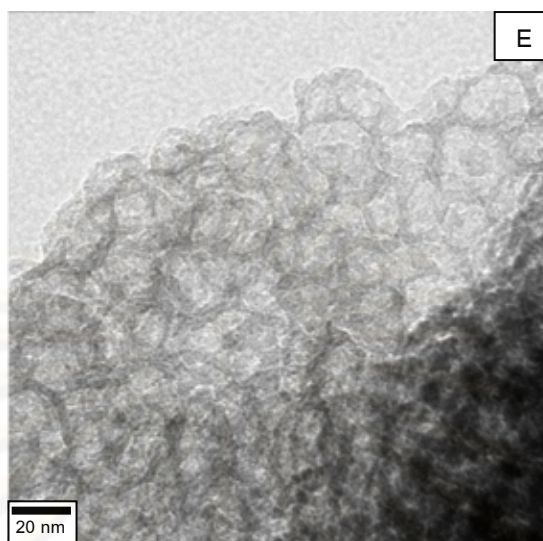


Figure 5.2 TEM images of mesoporous silica supports: MCM-41 observed perpendicular (A) and parallel (B) to the pores; SBA-15 observed perpendicular (C) and parallel (D) to the pores; MCF (E).

Figure 5.2 shows the TEM images of the mesoporous silica supports. The MCM-41 and SBA-15 mesoporous silica supports exhibited the hexagonal and long cylindrical pore structure. The structure of MCM-41 consists of parallel one-dimensional channels which form a hexagonal array [30] while SBA-15 exhibited the order hexagonal lattice (p6mm). The MCF material revealed the frame structure and larger pore size [21].

5.1.1.3 N₂ physisorption

N₂ physisorption was used to investigate the BET surface area, pore volume and average pore diameter for all the samples, pore volume and average pore diameter were calculated by means of BJH method. The results are present in Table 5.1. The first column had shows the specific surface area. It is indicated that all the mesoporous silica supports had high BET surface area $\geq 700 \text{ m}^2/\text{g}$ with MCM-41 had the highest surface area (834 m^2/g). Besides, the highest pore volume among the mesoporous silica was MCF material. The average pore diameter was in the order of MCF>SBA-15>MCM-41,

associated with the characteristic peak from XRD measurement, which determined to be 7.8 nm, 3.9 nm, and 2.7 nm, respectively.

Table 5.1 Pore characteristic of mesoporous silica supports

Samples	BET surface area (m ² /g)	Pore volume (cm ³ /g)	Pore diameter (nm)
MCM-41	834	0.87	2.7
SBA-15	810	0.84	3.9
MCF	700	1.12	7.8

The pore size distribution of mesoporous silica supports; MCM-41, SBA-15, and MCF from Figure 5.3 showed a narrow pore size for MCM-41 and SBA-15 materials. Meanwhile, the MCF showed a slightly larger pore size in comparison with those materials, similar to those reported in the literature [21].

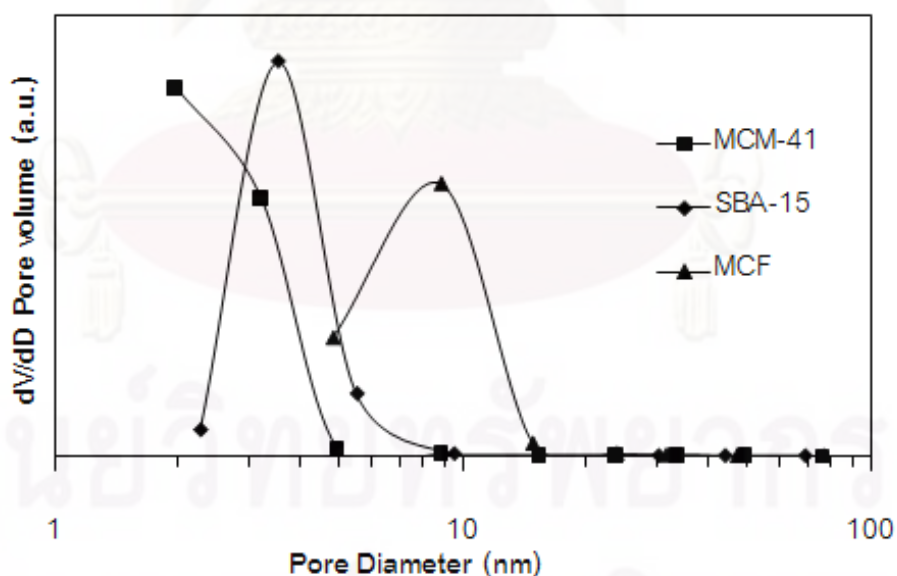


Figure 5.3 Pore size distribution of mesoporous silica supports

5.1.2 Pd nanoparticles characterization

Pd nanoparticles was prepared from reduction by solvent method using 1,4-dioxane as a reducing agent and redispersed in methanol. The Pd nanoparticles was characterized by means of TEM analysis in order to investigated the morphology of Pd particles.

The TEM images of Pd nanoparticles in methanol are shown in Figure 5.4 in the scale bar of 7 nm. The Pd nanoparticles demonstrated the mono dispersed in methanol with the average particles size of ca. 2.3 nm.

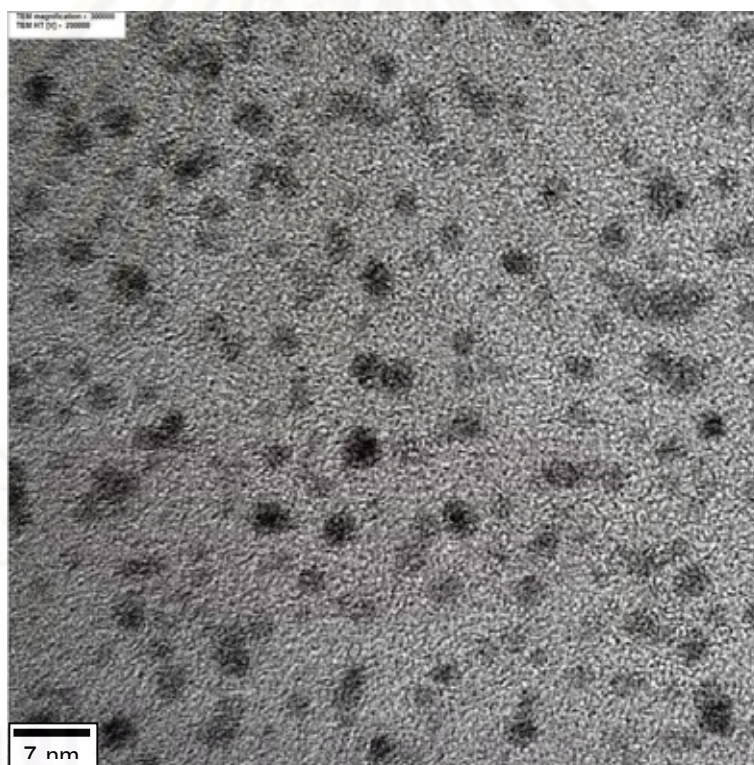


Figure 5.4 TEM image of Pd nanoparticles in methanol

These Pd nanoparticles were impregnated on the mesoporous silica supports by means of wet impregnation. The catalysts prepared by Pd(II)acetate solution impregnated on mesoporous silica by incipient wetness impregnation were used for comparison purposes.

5.1.3 Characterizations of the supported Pd catalysts

The mesoporous silica supported Pd catalysts were characterized by means of XRD, TEM, N₂ physisorption in order to investigate the structure and morphology after The CO-chemisorption, and AAS were employed to determine the amount of active Pd surface and the actual amount of Pd loading.

5.1.3.1 X-Ray Diffraction (XRD)

Figure 5.5 and Figure 5.6 show the characteristic peaks of the mesoporous silica after loading with Pd nanoparticles and Pd(II)acetate solution, respectively. The peak intensity for the mesoporous silica was decreased after loading of Pd nanoparticles [32, 33]. For the Pd/MCF catalyst, disappeared the characteristic peak, indicating less ordered hexagonal structure. This result could be explained by the mesopore of silica support was blocked with Pd species and/or the wall of mesoporous silica support was partly collapsed, resulting in a decrease in the reflection at low 2θ of Pd/MCF [32]. Besides, it may describe by the thermal instability of the support during the formation of Pd species [33]. The shift of diffraction peak to lower 2θ can be described as the thickening of the pore wall due to the transition-metal-promoted cross-linking of the amorphous silica walls [34], and resulting in a decrease of the interplanar spacing [15, 35].

ศูนย์วิทยทรัพยากร

จุฬาลงกรณ์มหาวิทยาลัย

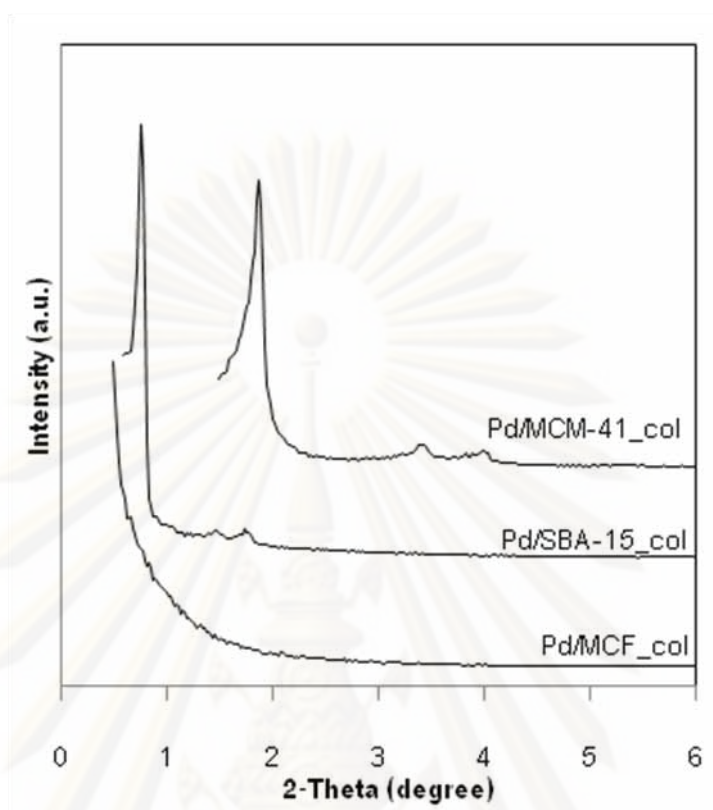


Figure 5.5 XRD patterns of Pd nanoparticles supported on mesoporous silica

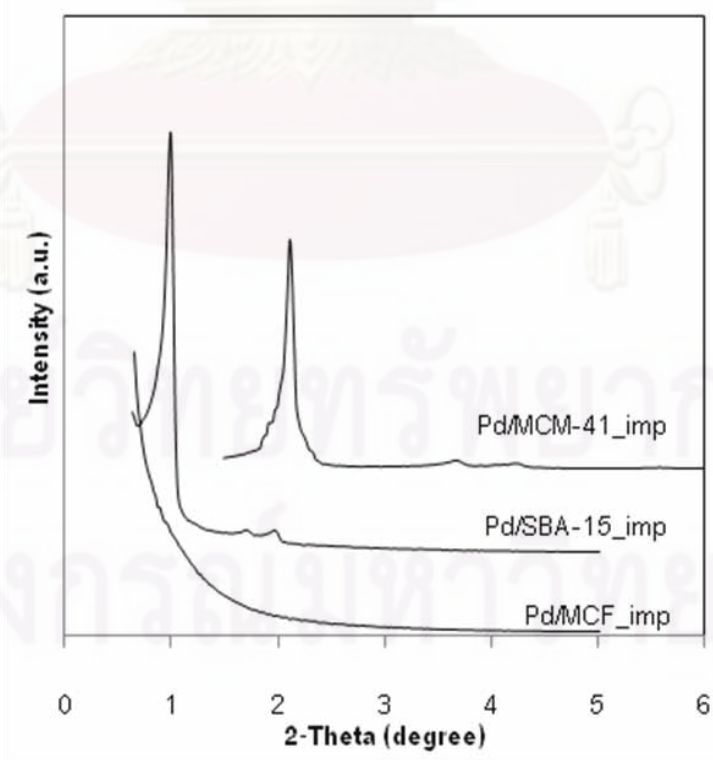


Figure 5.6 XRD pattern of Pd(II)acetate solution supported on mesoporous silica

The XRD pattern was recorded at higher 2-theta degree ($2\theta = 10-80^\circ$) in order to investigate the Pd on mesoporous silica supports. Figure 5.7 displayed XRD pattern of the catalysts prepared from Pd nanoparticles supported on mesoporous silica using wet impregnation method and the catalysts prepared from Pd(II)acetate solution using incipient wetness impregnation method. The Pd⁰ metal shows the reflection peak at 40.1° [12] for Pd/X_col catalysts. However, due to the low amount of Pd nanoparticles impregnated on the supports, the diffraction peak indicating Pd⁰ metal was not distinct.

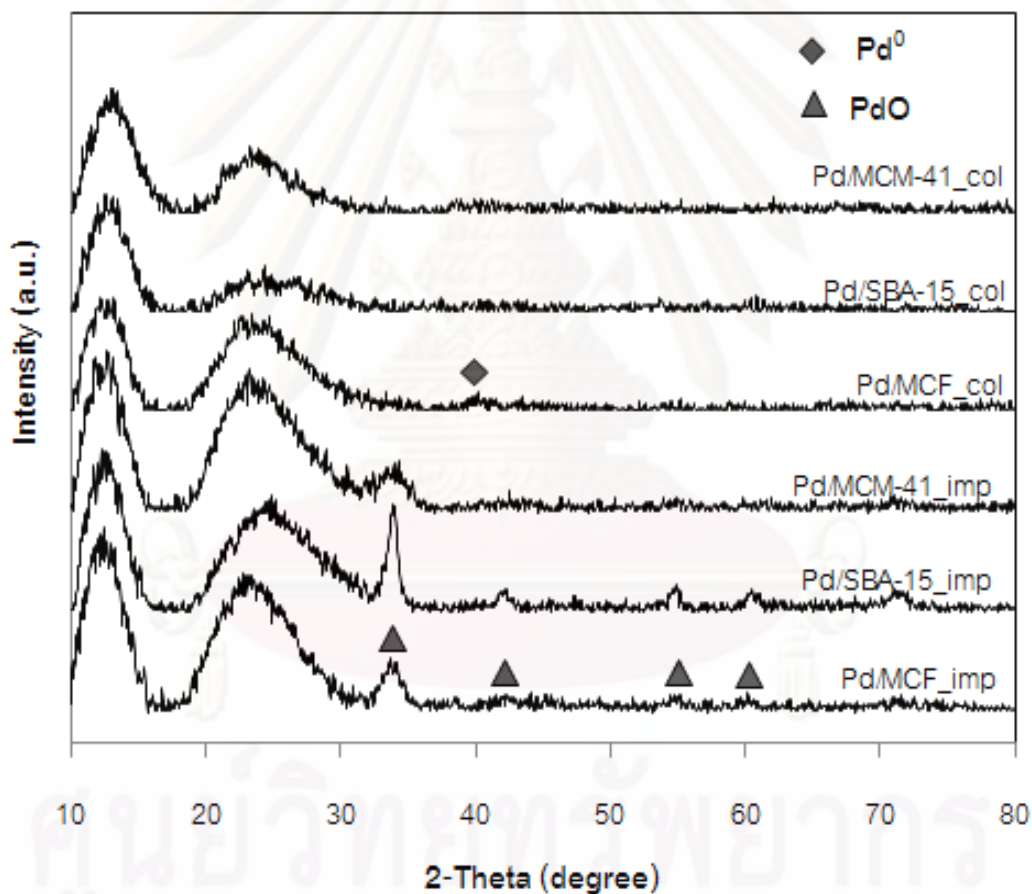


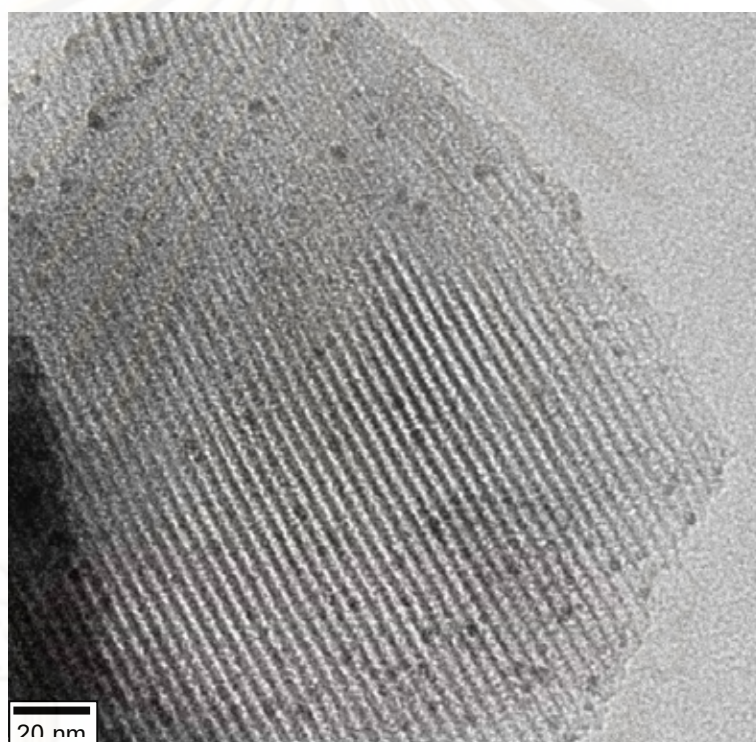
Figure 5.7 XRD pattern of the catalysts in the 2-theta range of $10-80^\circ$

The form of Pd oxide was detected from diffraction peaks at $2\theta = 33.8^\circ$, 42.0° , 54.8° , 60.7° , and 71.4° [12] for the catalysts prepared from Pd(II)acetate solution using incipient wetness impregnation method.

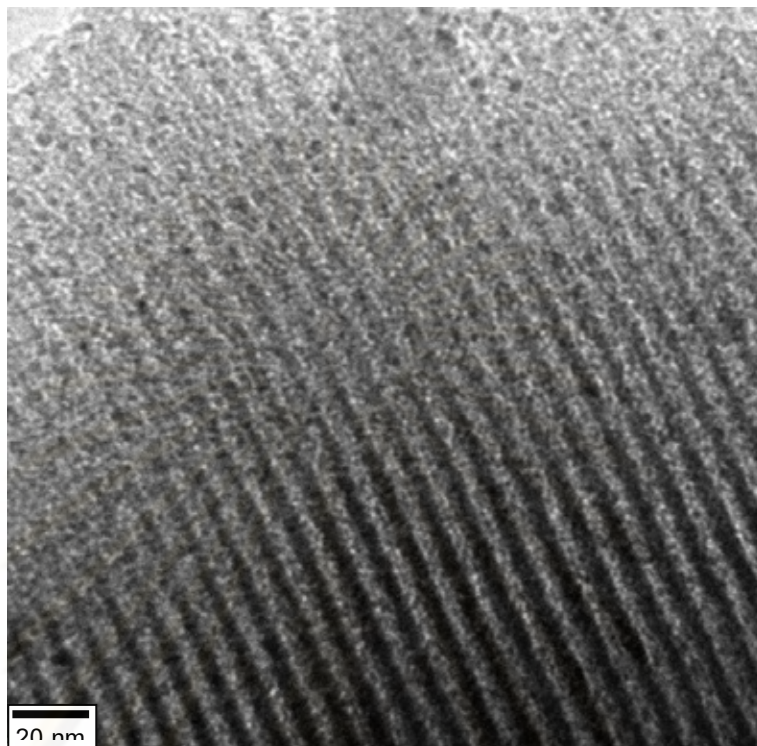
Furthermore, the broad diffraction peak at 2θ about 22° of all the catalysts (including the Pd/X_col and Pd/X_imp) was ascribable to the amorphous silica [36].

5.1.3.2 Transmission Electron Microscopy (TEM)

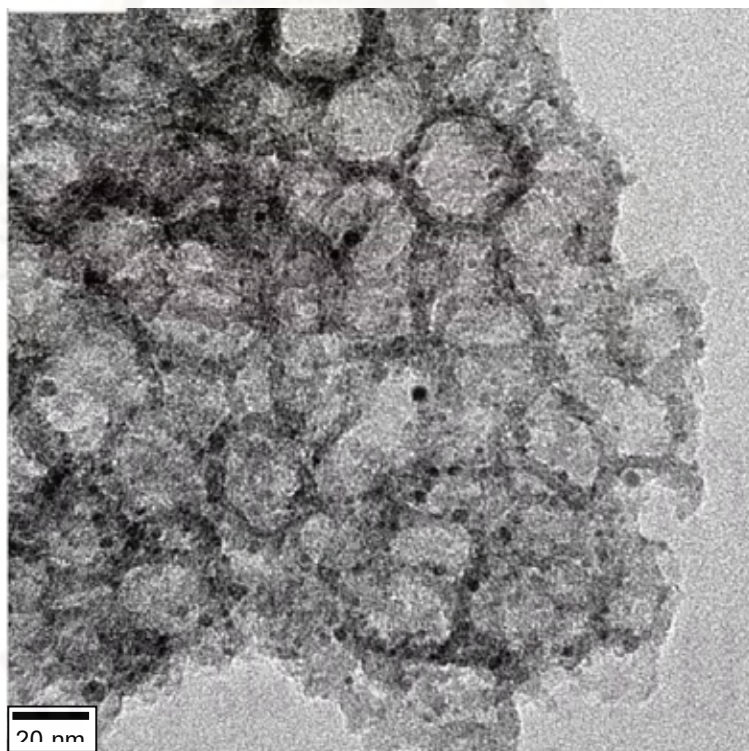
After supporting of Pd on mesoporous silica, the catalysts were investigated the Pd distribution, the location of Pd, and the Pd particles size by TEM method.



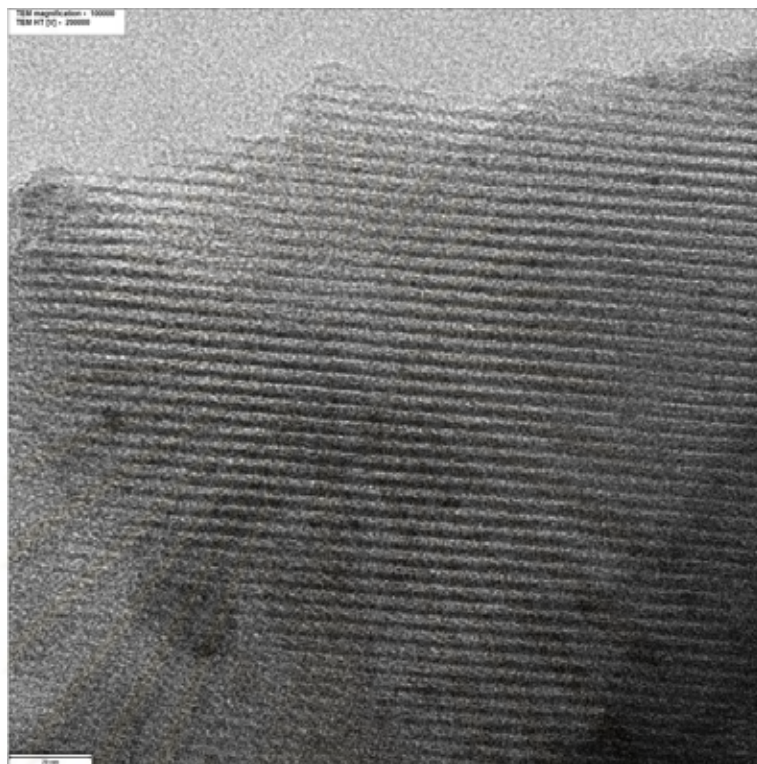
(a) Pd/MCM-41_col



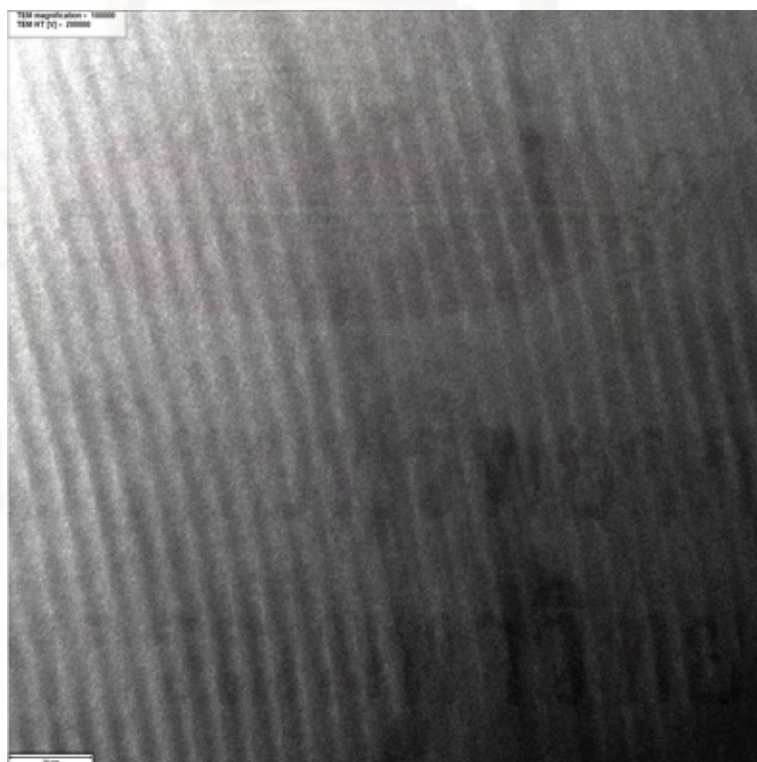
(b) Pd/SBA-15_col



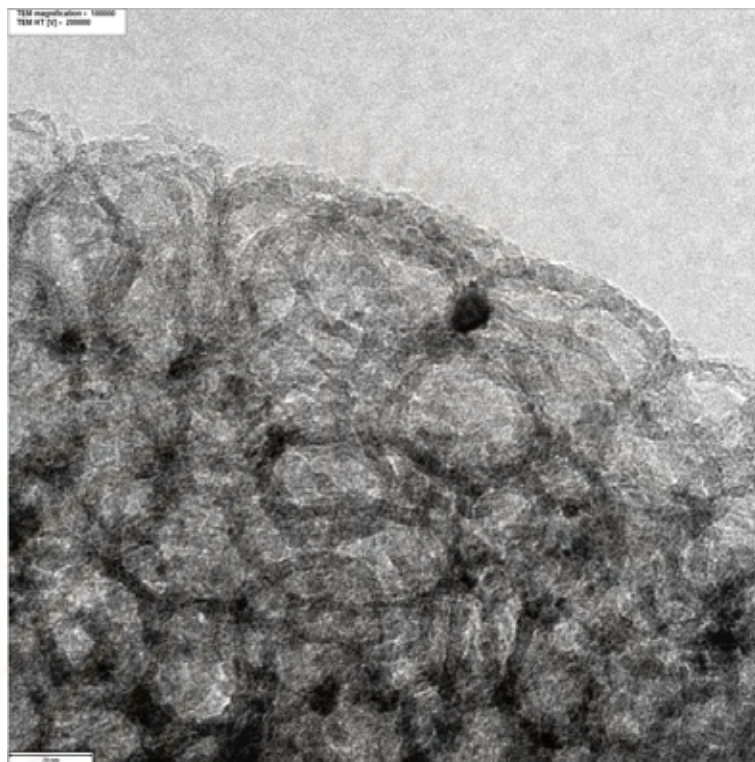
(c) Pd/MCF_col



(d) Pd/MCM-41_imp



(e) Pd/SBA-15_imp



(f) Pd/MCF_imp

Figure 5.8 TEM images of Pd nanoparticles supported on mesoporous silica before test in the hydrogenation reaction.

Figure 5.8 displays the TEM images of all the prepared catalysts. Figure 5.8(a) to Figure 5.8(c) were the catalysts prepared from Pd nanoparticles and Figure 5.8(d) to Figure 5.8(f) were the catalysts prepared from Pd(II)acetate solution with incipient wetness impregnation. The dark spots in all catalysts represented the Pd particles, except for the Pd/SBA-15_imp, it was shown as the long dark rod parallel to the pore. Although the deposition of Pd nanoparticles on mesoporous silica supports resulted in a decrease of XRD characteristic peak, the hexagonal, and frame structure of the MCM-41, SBA-15, and MCF were retained [37].

The average particles sizes of all the catalysts as measured by TEM analysis are reported in Table 5.2. In the case of Pd nanoparticles supported on mesoporous silica, no Pd cluster was observed in all the catalysts. The average particle size from TEM of Pd/MCM-41_col, Pd/SBA-15_col, and Pd/MCF_col were 2.4 nm, 2.3 nm, and 2.5 nm,

respectively, and similar to the average particle sizes of Pd colloid (2.3 nm), indicating that there was no sintering of Pd nanoparticles during catalyst preparation, and no effect of pore structure.

Table 5.2 Particle size from TEM analysis

sample	particle size, d_{TEM} (nm)
Pd/MCM-41_col	2.4
Pd/SBA-15_col	2.3
Pd/MCF_col	2.5
Pd/MCM-41_imp	4.0
Pd/SBA-15_imp	n.d.
Pd/MCF_imp	8.2

*n.d. = not determined

The catalysts prepared from Pd(II)acetate solution with incipient wetness impregnation showed the larger particles size, especially in the Pd/SBA-15_imp the size of Pd particle was not determined due to the shape of Pd was not spherical. The Pd particle size was increased when the pore diameter was larger. These results revealed that pore structure of the mesoporous silica supports affected the Pd particle size of those catalysts.

5.1.3.3 N₂ phisorption

The BET surface area, pore volume, and average pore diameter of the Pd catalysts supported on mesoporous silica supports are reported in Table 5.3.

Table 5.3 Pore characteristic of Pd supported on mesoporous silica.

Samples	BET surface area (m ² /g)	Pore volume (cm ³ /g)	Pore diameter (nm)
MCM-41	834	0.87	2.7
SBA-15	810	0.84	3.9
MCF	700	1.12	7.8
Pd/MCM-41_col	745	0.74	2.4
Pd/SBA-15_col	679	0.71	3.6
Pd/MCF_col	586	1.03	5.7
Pd/MCM-41_imp	813	0.87	2.7
Pd/SBA-15_imp*	867	0.81	3.9
Pd/MCF_imp*	727	1.81	7.6

* These mesoporous silica support were synthesized in a different batch from Pd/X_col catalysts.

After supporting of Pd nanoparticles with wet impregnation method (Pd/X_col), BET surface area, pore volume, and average pore diameters were decreased, indicating that some of the Pd particles may situated inside the pores. According to the catalysts prepared from Pd(II)acetate solution with incipient wetness impregnation method (Pd/X_imp). These catalysts were little change in BET surface area, pore volume, and average pore diameters, indicating the low dispersion of Pd particles.

The pore size distributions of all the catalysts are demonstrated in Figure 5.9. The mesoporous silica supports were shown in the solid line, while the Pd-supported catalysts shown in dash line. For MCM-41, the average pore diameter was out of the detection range, however, it seemed the pore size was not changed after Pd loading. For SBA-15, pore size and pore volume remained unchanged for the Pd/SBA-15_col

catalyst. The pore volume of Pd/SBA-15_imp, however, decreased due to the present of large Pd particle size as seen from TEM images. For MCF, after Pd loading the pore size distribution of MCF was wider, due probably to partial collapse of MCF structure. The results were consistent to XRD analysis.

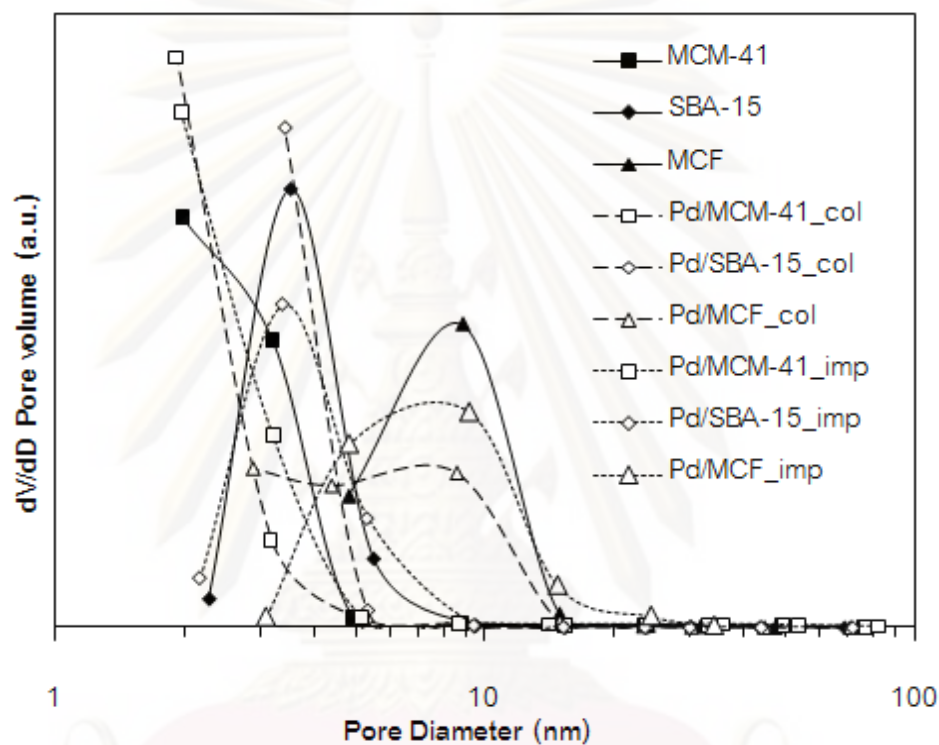


Figure 5.9 Pore size distribution of mesoporous silica before and after Pd loading.

5.1.3.4 CO-Pulse Chemisorption

The metal active sites measurement is based on CO chemisorption technique, the results are given in Table 5.4. The amount of CO chemisorption on the Pd/MCM-41_col, Pd/SBA-15_col, Pd/MCF_col, Pd/MCM-41_imp, Pd/SBA-15_imp, and Pd/MCF_imp were 16.1×10^{18} , 9.5×10^{18} , 10.6×10^{18} , 10.0×10^{18} , 2.2×10^{18} , and 7.6×10^{18} site/g catalyst, respectively. In addition, this result was similar to the order of Pd dispersion, but the Pd dispersion of Pd/SBA-15 was higher than Pd/MCF corresponding to the result from TEM characterization. The obtained average metal sizes of catalysts

which characterized by means of CO chemisorptions were larger than those from TEM analysis. The Pd sizes of Pd/MCM-41_col, Pd/SBA-15_col, and Pd/MCF_col, Pd/MCM-41_imp, Pd/SBA-15_imp, and Pd/MCF_imp were 3.2 nm, 3.4 nm, 4.4 nm, 7.6 nm, 23.9 nm, and 10.1 nm, respectively.

Table 5.4 CO chemisorptions results of prepared catalysts.

sample	Pd dispersion* (%)	Active site ($\times 10^{-18}$ site/g.cat)	metallic surface area (m^2/g of Pd)	particle size, d_{CO} (nm)
Pd/MCM-41_col	35.5	16.1	158	3.2
Pd/SBA-15_col	32.9	9.5	146	3.4
Pd/MCF_col	25.3	10.6	113	4.4
Pd/MCM-41_imp	14.80	10.0	66	7.6
Pd/SBA-15_imp	3.28	2.2	15	23.9
Pd/MCF_imp	11.16	7.6	50	10.1

* Based on the actual amount of Pd loading determined by atomic absorption spectroscopy.

5.1.3.5 X-ray Photoelectron Spectroscopy (XPS)

XPS was used to examine the binding energy and the surface composition of the catalysts. The results are reported in Table 5.5.

The Pd $3d_{5/2}$ of Pd/MCM-41_col, Pd/SBA-15_col, and Pd/MCF_col demonstrated the binding energy around 335 eV, corresponding to the Pd^0 , while the binding energy of Pd/MCM-41_imp, Pd/SBA-15_imp, and Pd/MCF_imp were around 337-338 eV, indicating the PdO corresponding to the unreduced sample. The shift of Pd $3d_{5/2}$ peak to higher binding energy in the case of Pd/SBA-15, indicating that the existence of more cationic Pd species [38].

Table 5.5 XPS results of all catalysts.

Sample	B.E. (ev)			Atomic conc. (%)			Pd/Si
	O 1s	Pd 3d	Si 2p	O 1s	Pd 3d	Si 2p	
Pd/MCM-41_col	532.4	334.9	102.9	51.65	0.23	22.62	0.0102
Pd/SBA-15_col	532.4	335.2	103	39.26	0.33	15.09	0.0219
Pd/MCF_col	532.4	334.7	102.8	48.75	0.17	21.6	0.0079
Pd/MCM-41_imp	533.7	337.7	104.1	67.57	0.04	32.39	0.0012
Pd/SBA-15_imp	535.6	338.9	106	68.74	0.06	31.21	0.0019
Pd/MCF_imp	533.6	336.9	104.1	64.08	0.01	30.02	0.0003

5.2 Catalytic test

The prepared catalysts were tested in liquid-phase selective hydrogenation of phenylacetylene under mild condition. In this study, 0.005 g of catalyst was reacting with 0.5 ml of phenylacetylene in ethanol under temperature of 40°C, 30 minute, and phenylacetylene: Pd molar ratio = 9700.

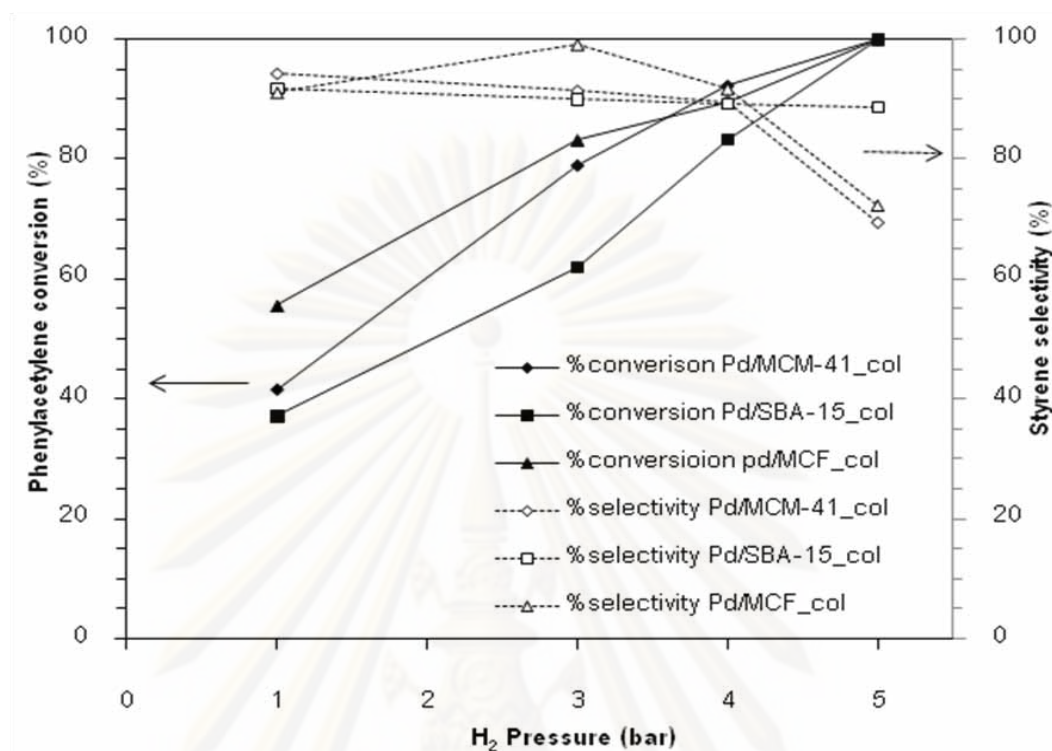


Figure 5.10 Conversion and selectivity of Pd/X_col catalysts in liquid phase selective hydrogenation of phenylacetylene at 40 °C, 30 min, H₂ pressure 1-5 bar.

The performance of catalysts was determined in term of phenylacetylene conversion and selectivity towards styrene. Figure 5.10 shows the catalytic activity of Pd/X_col catalysts in term of phenylacetylene conversion versus H₂ pressure along with selectivity toward styrene. The Pd/SBA-15_col exhibited lowest initial rate, according to the lower metal active sites as determined from CO chemisorption. At relatively low H₂ pressure (≤ 4 bar), all the prepared catalysts show high selectivity toward styrene ($\sim 90\%$). The total conversion of phenylacetylene was reached at H₂ pressure equal to 5 bar for all the catalysts. However, the selectivity toward styrene for all the catalysts was significantly decreased with increasing of H₂ pressure, except that of Pd/SBA-15_col that the styrene selectivity remained relatively high.

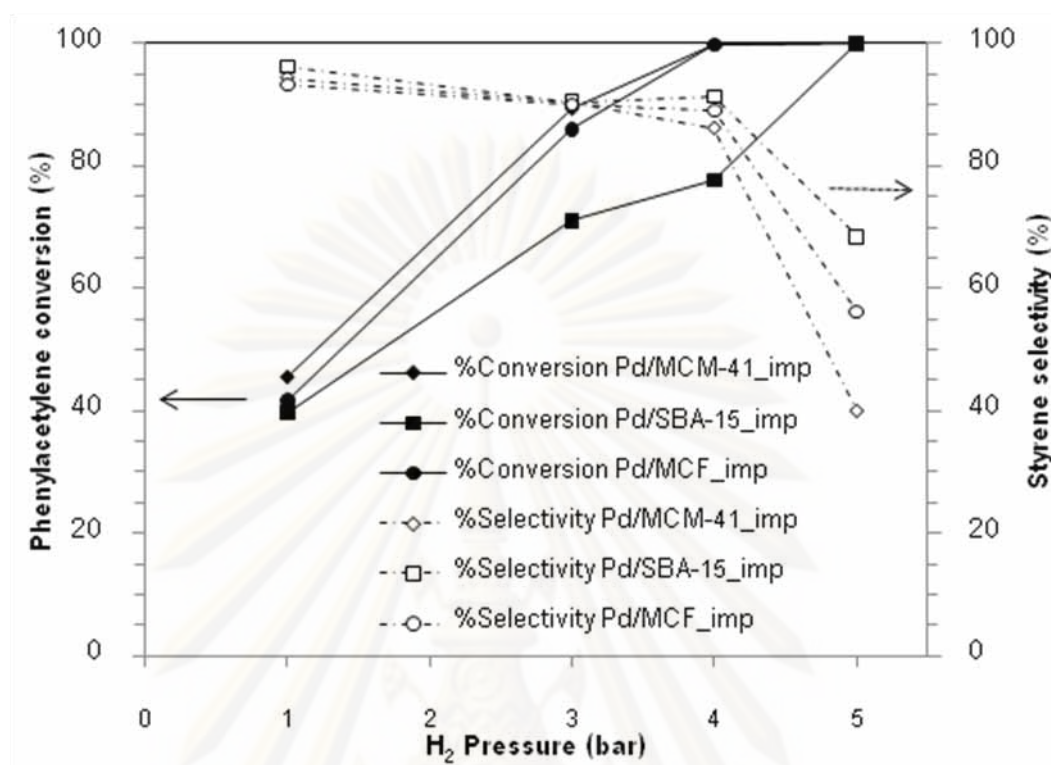


Figure 5.11 Conversion and selectivity of Pd/X_imp catalysts in liquid phase selective hydrogenation of phenylacetylene at 40°C, 30 min, H₂ pressure 1-5 bar.

The Pd/X_imp catalysts were tested in the liquid-phase selective hydrogenation of phenylacetylene under the similar reaction conditions of those of the Pd/X_col catalysts and the results are present in Figure 5.11. The results of the Pd/X_imp catalysts were similar to those obtained from the Pd/X_col catalysts in with the Pd/SBA-15_imp showed slow initial rate. At the H₂ pressure of 4 bar, the phenylacetylene conversion was reached to 100% in the Pd/MCM-41_imp and Pd/MCF_imp, while Pd/SBA-15_imp had a phenylacetylene conversion about 75% and reached 100% conversion at 5 bar. The selectivity toward styrene of all the catalysts was decreased with increasing the H₂ pressure, with the lowest decreased for the Pd/SBA-15_imp catalyst.

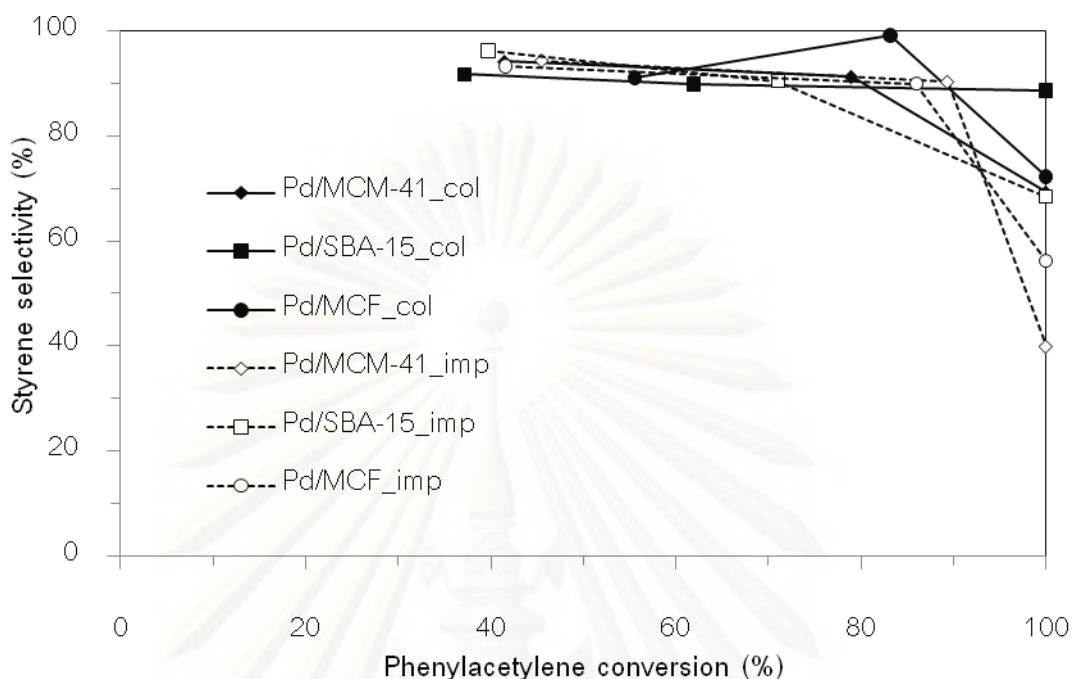


Figure 5.12 Performance curves of all the catalysts.

Figure 5.12 demonstrated the performance of all catalysts in the liquid-phase selective hydrogenation of phenylacetylene. Although, the Pd/SBA-15 showed the highest styrene selectivity in each preparation procedure, the Pd/SBA-15_col catalysts showed the highest styrene selectivity at completed phenylacetylene conversion in comparisons with all the catalysts in the order Pd/SBA-15_col > Pd/MCF_col > Pd/MCM-41_col \approx Pd/SBA-15_imp > Pd/MCF_imp > Pd/MCM-41_imp. These results explained by the location of Pd particle, Pd particle size, and the pore structure. The pores of mesoporous silica supports should be large enough that the Pd particles were located inside the pore but not too large in order to provide the beneficial effect for improving the styrene selectivity during the selective hydrogenation of phenylacetylene [38].

จุฬาลงกรณ์มหาวิทยาลัย

Table 5.6 Initial reaction results of the catalysts.

Catalysts	Conversion (%)	Selectivity (%)	TOF (s^{-1})
Pd/MCM-41_col	41	94	7.9
Pd/SBA-15_col	37	92	12
Pd/MCF_col	56	91	16
Pd/MCM-41_imp	46	94	13.9
Pd/SBA-15_imp	40	96	55.2
Pd/MCF_imp	42	93	16.7

Table 5.6 shows phenylacetylene conversion and styrene selectivity for Pd/X_col and Pd/X_imp under reaction conditions of H_2 pressure 1 bar, $40^\circ C$, 30 min. It was observed that phenylacetylene conversion increased in the order Pd/MCF_col > Pd/MCM-41_imp > Pd/MCF_imp > Pd/MCM-41_col > Pd/SBA-15_imp > Pd/SBA-15_col with little effect on the styrene selectivity. The Pd/SBA-15_col had the lowest hydrogenation activity, due probably to some of the Pd metals were located inside the mesopore and may limit the adsorption of phenylacetylene or desorption of the products.

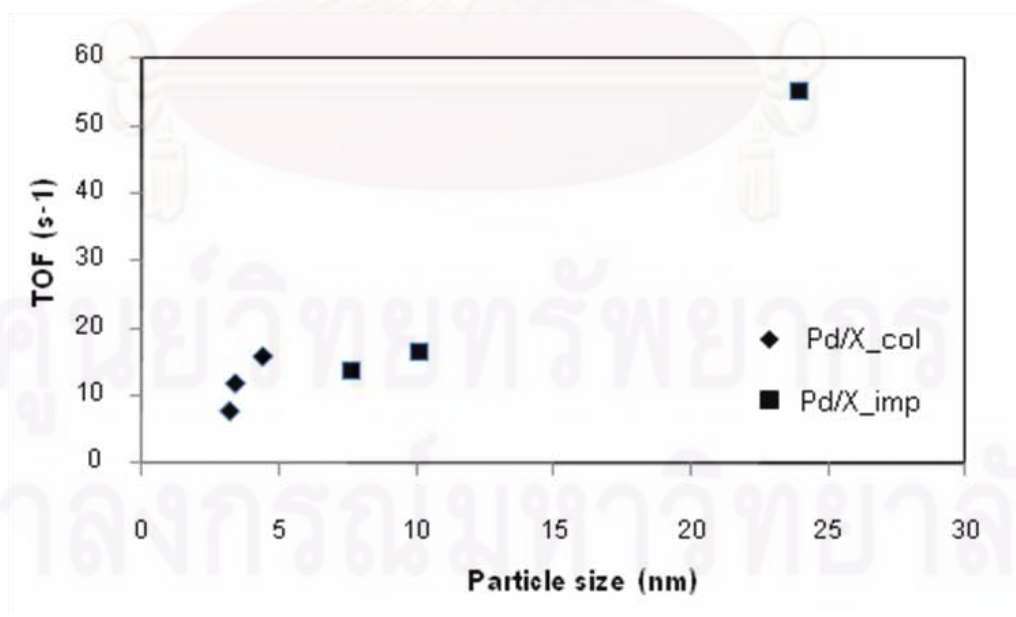


Figure 5.13 Relation between particle sizes and TOF in the first cycle of selective hydrogenation of phenylacetylene.

The specific activity of all catalysts were calculated in term of turn over frequencies (TOF) based on the number of palladium sites measured by irreversible CO chemisorptions. Figure 5.13 shows TOF versus Pd⁰ metal particle size. As can be observed, the TOF increased with increasing metal particle size so the reaction was structure sensitive. The previous studies have reported that palladium with larger particle size was more active in selective hydrogenation than smaller ones [3, 19]. However, the particle size had a limiting value at the diameter of 11 nm, above this size the reaction is not size-dependent [39].

The catalysts were tested in the selective hydrogenation of phenylacetylene for four cycles to determine the stability of the catalysts and the catalysts recyclability performance. The recyclability was summarized in Table 5.7. The catalytic behavior after four cycles of reutilization was not much altered from the first cycle, especially in term of the selectivity toward styrene of Pd/X_col catalysts. Meanwhile, the Pd/MCM-41_imp catalysts shown largest decreased in selectivity toward styrene.

Considering the phenylacetylene conversion of Pd-supported catalysts after four cycles reaction, the Pd/MCM-41_col showed higher decrease in phenylacetylene conversion in comparison with Pd/SBA-15_col and Pd/MCF_col.

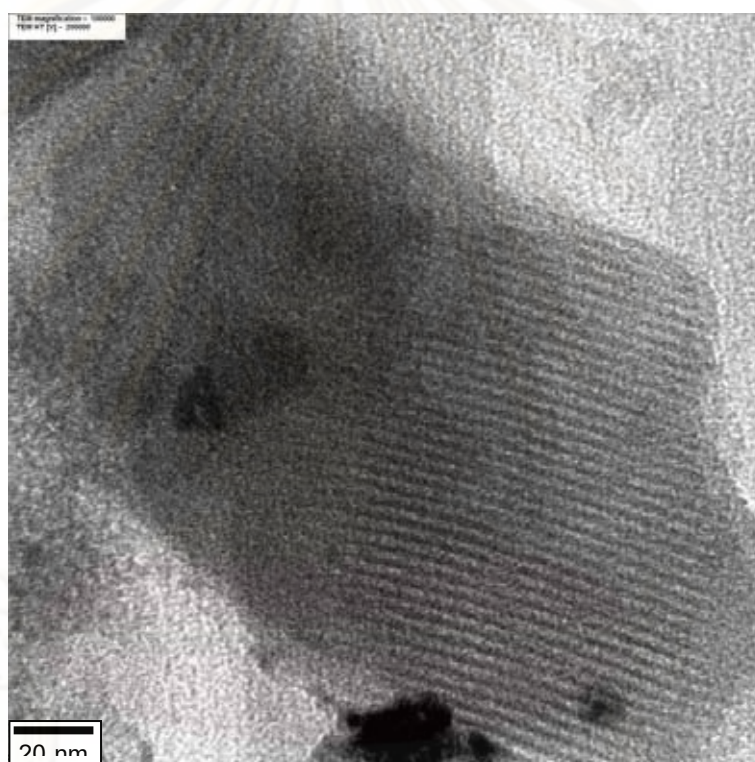
Table 5.7 Recyclability of Pd/MCM-41, Pd/SBA-15, and Pd/MCF for four cycles

catalyst	Cycle 1		Cycle 4	
	conversion	selectivity	conversion	selectivity
Pd/MCM-41_col	81	93	76	93
Pd/SBA-15_col	72	93	74	91
Pd/MCF_col	89	92	86	91
Pd/MCM-41_imp	79	89	100	50
Pd/SBA-15_imp	78	94	94	92
PD/MCF_imp	72	89	100	85

5.3 Characterization of the samples after reaction

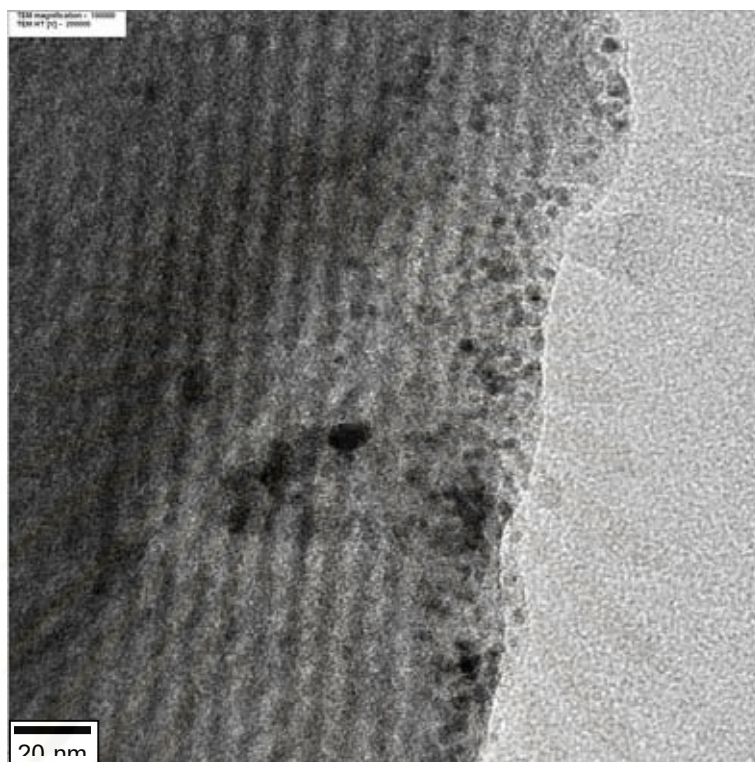
The catalysts were tested in the liquid-phase selective hydrogenation of phenylacetylene for four cycles and investigated the structure of mesoporous silica supports and the Pd particles using TEM and AAS techniques.

5.3.1 Transmission Electron Microscopy (TEM)

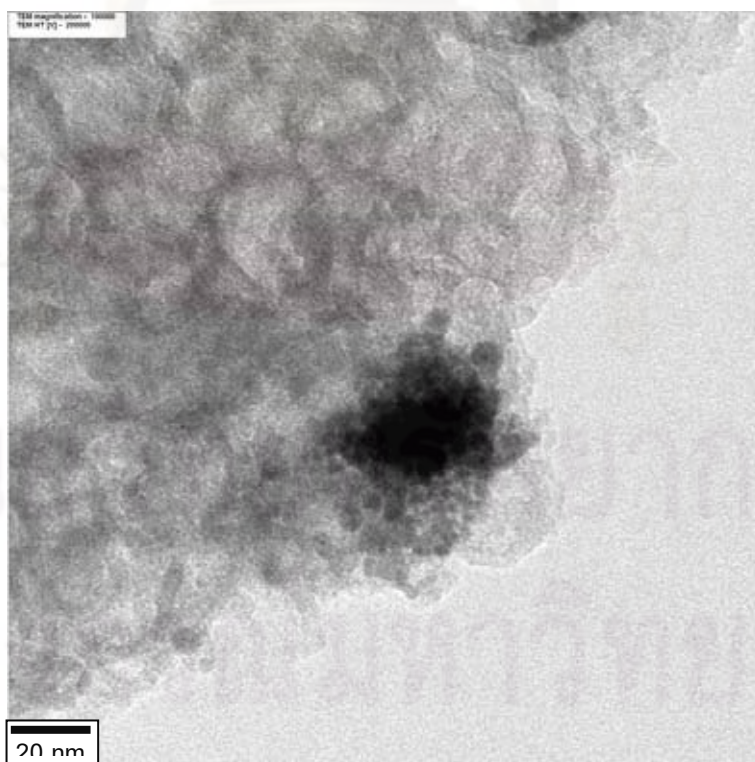


(a) Pd/MCM-41_col

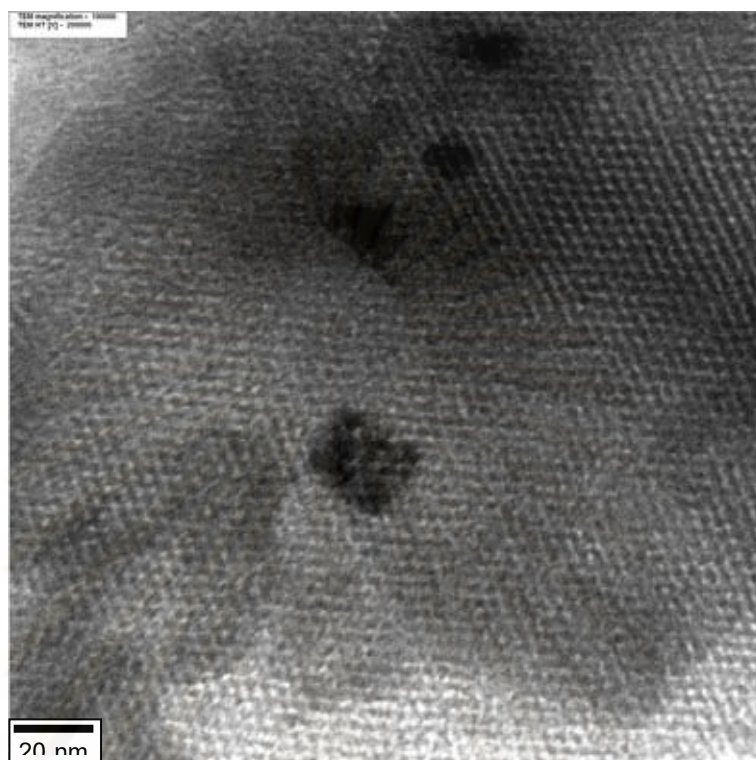
ศูนย์วิทยทรัพยากร
จุฬาลงกรณ์มหาวิทยาลัย



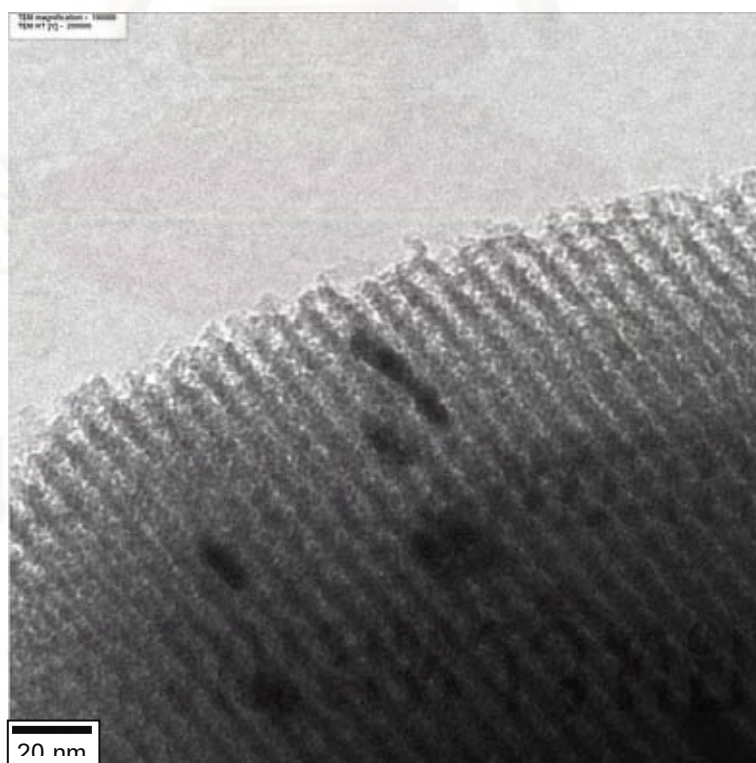
(b) Pd/SBA-15_col



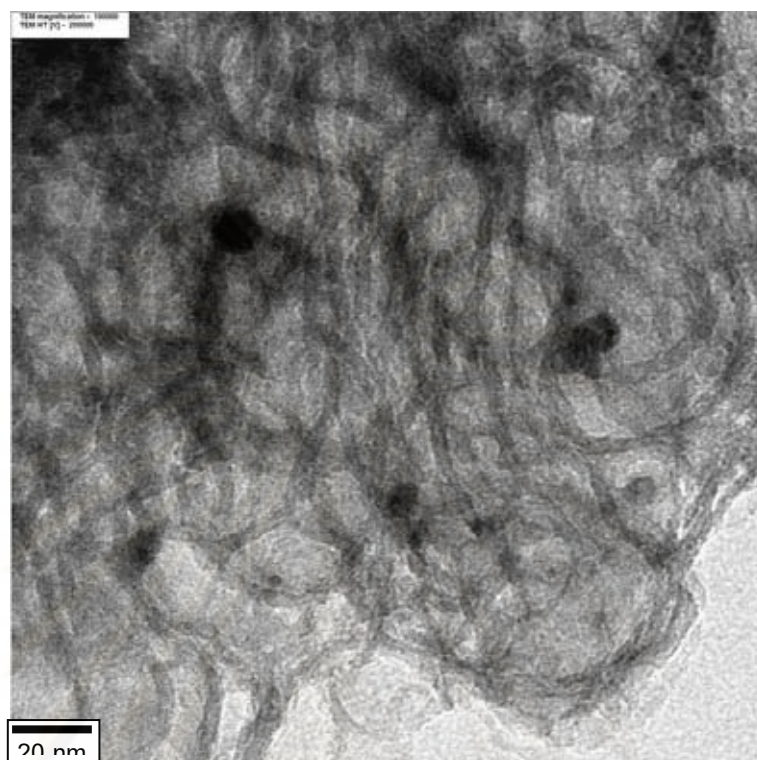
(c) Pd/MCF_col



(d) Pd/MCM-41_imp



(e) Pd/SBA-15_imp



(f) Pd/MCF_imp

Figure 5.14 TEM images of the catalysts after recycling in selective hydrogenation of phenylacetylene for four cycles.

TEM images of the catalysts after reaction for four cycles were shown in Figure 5.14. The structures of MCM-41 and SBA-15 in two cases were partly destroyed, while SBA-15 was retained. The Pd particles in the Pd/MCM-41_X and Pd/MCF_X catalysts were aggregation, result in the larger Pd size. However, the Pd/SBA-15_X exhibited the similar Pd size and shape comparative with before reaction.

5.3.2 Atomic Absorption Spectroscopy (AAS)

The Pd content in the bulk of catalysts was characterized using atomic absorption spectroscopy (AAS) technique and present in Table 5.8.

Table 5.8 Actual amount of Pd in the samples before and after reaction for four cycles from AAS technique

sample	Pd content (wt%)		% Metal loss
	before reaction	after reaction	
Pd/MCM-41_col	0.80	0.59	26.25
Pd/SBA-15_col	0.51	0.27	47.06
Pd/MCF_col	0.74	0.56	24.32
Pd/MCM-41_imp	1.20	0.69	42.50
Pd/SBA-15_imp	1.20	0.91	24.17
Pd/MCF_imp	1.20	0.89	25.83

In the preparation procedure, all the catalysts were prepared for Pd loading of ca. 1 wt%. However, the actual amounts of Pd in the Pd nanoparticles catalysts were less than the design amount. These results indicated that some of Pd may be leached during the preparation. The catalysts prepared from Pd(II)acetate solution showed the higher Pd content at 1.20 wt%.

After the reaction for four cycles, some of the Pd metals were leached from the mesoporous silica due probably to the weak-interaction between Pd metal and the supports. The Pd/SBA-15_col and Pd/MCM-41_imp showed the largest decreased in the Pd metal, while the other catalysts showed the decreased about 25%.

CHAPTER VI

CONCLUSIONS AND RECOMMENDATIONS

In this chapter composed of two sections, section 6.1 reveals the conclusions obtained from the experimental results of the prepared catalysts and the catalytic studies in the liquid phase selective hydrogenation of phenylacetylene to styrene. Additionally, recommendations for further study are given in section 6.2.

6.1 Conclusions

1. All the mesoporous silica supports had high BET surface area in the range of 700 to 834 m²/g. The average pore diameters were determined to be 2.7, 3.9, and 7.8 nm for MCM-41, SBA-15, and MCF, respectively.

2. The Pd/SBA-15 showed the lowest metal active sites as determined from CO chemisorption for both of the preparation methods compared to Pd/MCM-41 and Pd/MCF catalysts, indicating that the Pd particles were located inside the mesopore more than the other catalysts.

3. Pore structure of mesoporous silica supports did not affect the Pd particle size of Pd/X_col catalysts. For the Pd/X_imp, the Pd particle size was increased with increasing pore diameter of the supports, however, the largest Pd particles were obtained on the Pd/SBA-15_imp, they were formed in a long cylindrical shape similar to the SBA-15 structure.

4. The liquid-phase selective hydrogenation of phenylacetylene was tested for all the catalysts under mild conditions. At the complete phenylacetylene conversion, the selectivity toward styrene was slightly decreased in the case of Pd/X_col catalysts, while the Pd/X_imp showed significant decrease in the styrene selectivity.

5. The higher styrene selectivity of Pd/SBA-15_col and Pd/SBA-15_imp catalysts were attributed to the formation of Pd particles inside the pores of SBA-15 structure.

6. The Pd/X_col exhibited high catalyst stability during the recyclability test for four cycles of reaction. The catalysts prepared from Pd(II)acetate solution, on the other hand, showed higher phenylacetylene conversion and lower styrene selectivity in some cases (Pd/MCM-41_imp).

6.2 Recommendations

1. The catalysts prepared from both Pd nanoparticles and Pd(II)acetate solution should be improved in terms of the interaction between Pd metal and mesoporous silica supports.
2. The simultaneous synthesis of Pd nanoparticles and mesoporous silica should be investigated.
3. The catalysts should be investigated using other techniques to confirm the bonding of Pd metal and supports such as FT-IR.
4. The atomic absorption spectroscopy (AAS) results should be confirmed and the recyclability should be studied more than four cycles of run.

REFERENCES

- [1] Domínguez-Domínguez, S., and others. Semihydrogenation of phenylacetylene catalyzed by metallic nanoparticles containing noble metals. Journal of catalysis 243 (2006): 74–81.
- [2] Domínguez-Domínguez, S., and others. Semihydrogenation of phenylacetylene catalyzed by palladium nanoparticles supported on carbon materials. Journal of Physical Chemistry C 112 (2008): 3827-3834.
- [3] Domínguez-Domínguez, S., and others. Inorganic materials as supports for palladium nanoparticles: Application in the semi-hydrogenation of phenylacetylene. Journal of Catalysis 257 (2008): 87–95.
- [4] Vergunst, T., and others. Optimization of Geometric Properties of a Monolithic Catalyst for the Selective Hydrogenation of Phenylacetylene. Ind. Eng. Chem. Res. 40 (2001): 2801-2809.
- [5] Huang, X., and others. Phenylacetylene hydrogenation in a three-phase catalytic packed-bed reactor: experiments and model. Chemical Engineering Science 58 (2003): 3465 – 3471.
- [6] Gucci, L., and others. Pumice-Supported Cu–Pd Catalysts: Influence of Copper on the Activity and Selectivity of Palladium in the Hydrogenation of Phenylacetylene and But-1-ene. Journal of Catalysis 182 (1999): 456–462.
- [7] Marin-Astorga, N., and others. A comparative study of Pd supported on MCM-41 and SiO₂ in the liquid phase hydrogenation of phenyl alkyl acetylenes mixtures. Journal of Molecular Catalysis A: Chemical 231(2005): 67-74.
- [8] Marin-Astorga, N., and others. Stereoselective hydrogenation of phenyl alkyl acetylene on pillared clays supported palladium catalysts. Journal of Molecular Catalysis A: Chemical 226 (2005): 81-88.
- [9] Molnar, A., and others. Hydrogenation of carbon-carbon multiple bonds: chemo-, regio- and stereo-selectivity. Journal of Molecular Catalysis A: Chemical 173 (2001): 185–221.

- [10] David Jackson, S., and Shaw, L.A. The liquid-phase hydrogenation of phenyl acetylene and styrene on a palladium/carbon catalyst. Applied Catalysis A 134 (1996): 91-99.
- [11] Lopez, T., and others. Structure of Pd/SiO₂ sol-gel and impregnated catalysts. Journal of Sol-Gel Science and Technology 1 (1994): 193-203.
- [12] Panpranot, J., and others. A comparative study of Pd/SiO₂ and Pd/MCM-41 catalysts in liquid-phase hydrogenation. Catalysis Communications 5 (2004): 583–590.
- [13] Panpranot, J., and others. Impact of palladium silicide formation on the catalytic properties of Pd/SiO₂ catalysts in liquid-phase semihydrogenation of phenylacetylene. Journal of Molecular Catalysis A: Chemical 261 (2007): 29–35.
- [14] Marin-Astorga, N., and others. Alkynes hydrogenation over Pd-supported catalysts. Catalysis Letters 91 (2003): 115-121.
- [15] Papp, A., and others. Catalytic investigation of Pd particles supported on MCM-41 for the selective hydrogenations of terminal and internal alkynes. Applied Catalysis A: General 289 (2005): 256-266.
- [16] Marin-Astorga, N., and others. Mesostructured silicas as supports for palladium-catalyzed hydrogenation of phenylacetylene and 1-phenyl-1-hexyne to alkenes. Journal of Molecular Catalysis A 247 (2006):145–152.
- [17] Du, F., and others. Preparation and characterization of Pd/Si-MCM-41 with high hydrogenation activity. Journal of Porous Material 15 (2008): 613-617.
- [18] Del Angel, G., and Benitez, J.L. Selective hydrogenation of phenylacetylene on Pd/Al₂O₃: Effect of the addition of Pt and particle size. Reaction Kinetics and Catalysis Letters 51 (1993): 547-553.
- [19] Weerachawanasak, P., and others. Effect of strong metal-support interaction on the catalytic performance of Pd/TiO₂ in the liquid-phase semihydrogenation of phenylacetylene. Journal of Catalysis 262 (2009): 199-205.

- [20] Weerachawanasak, P., and others. A comparative study of strong metal-support interaction and catalytic behavior of Pd catalysts supported on micron- and nano-sized TiO₂ in liquid-phase selective hydrogenation of phenylacetylene. Journal of Molecular Catalysis A: Chemical 279 (2008): 133-139.
- [21] Chouyyok, W., and others. Effects of pH and pore characters of mesoporous silicas on horseradish peroxidase immobilization. Journal of Molecular Catalysis B: Enzymatic 56 (2009): 246–252.
- [22] Zhao, D., and others. Triblock copolymer syntheses of mesoporous silica with periodic 50 to 300 angstrom pores. Science 279 (1998): 548-552.
- [23] Lettow, J. S., and others. Hexagonal to mesocellular foam phase transition in polymer-template mesoporous silica. Langmuir 16 (2000): u291-8295.
- [24] Arena, F., and others. Palladium catalysts supported on oligomeric aramides in the liquid-phase hydrogenation of phenylacetylene. Journal of Molecular Catalysis A 110 (1996): 235-242.
- [25] Musolino, M.G., and others. Hydrogenation versus isomerization in α,β -unsaturated alcohols reactions over Pd/TiO₂ catalysts. Journal of Molecular Catalysis 208 (2004): 219–224.
- [26] Panpranot, J., and others. A comparative study of liquid-phase hydrogenation on Pd/SiO₂ in organic solvents and under pressurized carbon dioxide:Activity change and metal leaching/sintering. Journal of Molecular Catalysis A 253 (2006): 20–24.
- [27] Mastalir, A., and others. In situ generation of Pd nanoparticles in MCM-41 and catalytic applications in liquid-phase alkyne hydrogenations. Journal of Molecular Catalysis A: Chemical 264 (2007):170–178.
- [28] Li, H., and others. Ni-B amorphous alloy deposited on an aminopropyl and methyl co-functionalized SBA-15 as a highly active catalyst for chloronitrobenzene hydrogenation. Journal of Molecular Catalysis A: Chemical 307 (2009): 105-114.

- [29] Karakoulia, S. A., and others. Preparation and characterization of vanadia catalysts supported on non-porous, microporous and mesoporous silicates for oxidative dehydrogenation of propane (ODP). Microporous and Mesoporous Materials 110 (2008): 157-166.
- [30] Ryoo, Ry., and Jun, Sh. Improvement of hydrothermal stability of MCM-41 using salt effects during the crystallization process. Journal of Physical Chemistry B 101 (1997): 317-320.
- [31] Broyer, M., and others. Influence of aging, thermal, hydrothermal, and mechanical treatments on the porosity of MCM-41 mesoporous silica. Langmuir 18 (2002): 5083-5091.
- [32] Liu, Y., and others. Highly active methanol decomposition catalyst derived from Pd-hydroxalate dispersed on mesoporous silica. Catalysis Letters 66 (2000): 205-213.
- [33] Hao, X. Y., and others. A novel approach to prepare MCM-41 supported CuO catalyst with high metal loading and dispersion. Microporous and Mesoporous Materials 88 (2006): 38-47.
- [34] Hu, Sh., and others. A non-sodium synthesis of highly ordered V-MCM-41 and its catalytic application in isomerization. Catalysis Letters 129 (2009): 478-485.
- [35] Cho, D. H., and others. Characterization and catalytic activities of MoMCM-41. Catalysis Letters 64 (2000): 227-232.
- [36] Lui, J.L., and others. Ce-promoted Ru/SBA-15 catalysts prepared by a "two solvents" impregnation method for selective hydrogenation of benzene to cyclohexene. Applied Catalysis A: General 353 (2009): 282-287.
- [37] Zheng, Sh., & Gao, L., Synthesis and characterization of Pt, Au or Pd clusters deposited titania-modified mesoporous silicate MCM-41. Materials Chemistry and Physics 78 (2002): 512-517.
- [38] Panpranot, J., and others. Impact of the silica support structure on liquid-phase hydrogenation on Pd catalysts. Industrial & Engineering Chemistry Research 43 (2004): 6014-6020.

- [39] Fox, E. B., and others. Characterization of CeO₂-supported Cu-Pd bimetallic catalyst for the oxygen-assisted water-gas shift reaction. Journal of Catalysis 260 (2008): 358-370.



ศูนย์วิทยทรัพยากร
จุฬาลงกรณ์มหาวิทยาลัย



APPENDICES

ศูนย์วิทยทรัพยากร
จุฬาลงกรณ์มหาวิทยาลัย

APPENDIX A

CALCULATION FOR CATALYST PREPARATION

The calculation shown below is for 1%Pd on mesoporous silica supports. The support weight used for all preparation is 2 g.

Based on 100 g of catalyst used, the composition of the catalyst will be as follows:

$$\begin{aligned} \text{Palladium} &= 1 \text{ g} \\ \text{Mesoporous silica} &= 100-1 = 99 \text{ g} \end{aligned}$$

For 2 g of mesoporous silica

$$\text{Palladium required} = (2 \times 1) / 99 = 0.0202 \text{ g}$$

$$\text{Molecular weight of Pd(II)acetate} = 224.42 \text{ g/mol}$$

Then, Pd(II)acetate was taken

$$\begin{aligned} &= \frac{\text{M.W. of Pd(II)acetate} \times \text{Weight of Pd required}}{\text{M.W. of Pd}} \\ &= \frac{224.42 \times 0.0202}{106.42} \\ &= 0.0426 \text{ g} \end{aligned}$$

Palladium(II)acetate 0.0426 g was dissolved in acetone, which required appropriated amount with pore volume of each mesoporous silica support for the requirement of incipient wetness impregnation method.

APPENDIX B

CALCULATION FOR CO-CHEMISORPTION

Calculation of the metal active sites, metal dispersion, active metal surface area, and average crystallite size of the catalyst measured by CO-chemisorption is as follows:

Volume of active gas dosed from a loop (V_{inj})

$$V_{inj} = V_{loop} \times \frac{T_{std}}{T_{amb}} \times \frac{P_{amb}}{P_{std}} \times \frac{\%A}{100\%}$$

Example: Volume Dosed Using 100% Active Gas

V_{loop}	=	loop volume injected	86	μL
T_{amb}	=	ambient temperature	295	K
T_{std}	=	standard temperature	273	K
P_{amb}	=	ambient pressure	743	mmHg
P_{std}	=	standard pressure	760	mmHg
$\%A$	=	%active gas	100	%

$$V_{inj} = 86\mu\text{L} \times \frac{273\text{K}}{295\text{K}} \times \frac{743\text{mmHg}}{760\text{mmHg}} \times \frac{100\%}{100\%} = 77.8062\mu\text{L}$$

Volume chemisorbed (V_{ads})

$$V_{ads} = \frac{V_{inj}}{m} \times \sum_{i=1}^n \left[1 - \frac{A_i}{A_f} \right]$$

Example: CO Chemisorption on 1wt% Pd/MCM-41_col

V_{inj}	=	volume injected	77.8062	μL
m	=	mass of sample	0.1502	g
A_f	=	area of peak last peak	0.01499	

Peak	A_i	$1-A_i/A_f$
1	0.00527	0.6484
2	0.00681	0.5457
3	0.01495	0.0027
4	0.01499	0

$$V_{ads} = 0.5976 \text{ cm}^3/\text{g}$$

% Metal dispersion

$$\%D = S_f \times \frac{V_{ads}}{V_g} \times \frac{M.W.}{\%M} \times 100\% \times 100\%$$

Example: %Dispersion of 1wt% Pd/MCM-41_col

S_f	=	stoichiometer factor, CO on Pd	1	
V_{ads}	=	volume adsorbed	0.5976	cm^3/g
V_g	=	molar volume of gas at STP	22414	cm^3/mol
m.w.	=	molecular weight of the metal	106.42	g/mol
%M	=	weight percent of the active metal	0.8	%

$$\%D = 1 \times \frac{0.5976 \text{ cm}^3/\text{g}}{22414 \text{ cm}^3/\text{mol}} \times \frac{106.42 \text{ g/mol}}{0.8\%} \times 100\% \times 100 = 35.47\%$$

Pd active sites

$$Pd \text{ active sites} = S_f \times \frac{V_{ads}}{V_g} \times N_A$$

S_f	=	stoichiometry factor, CO on Pd	1
V_{ads}	=	volume adsorbed	0.5976 cm ³ /g
V_g	=	molar volume of gas at STP	22414 cm ³ /mol
N_A	=	Avogadro's number	6.023 × 10 ²³ molecules/mol

$$Pd \text{ active sites} = 1 \times \frac{0.5976 \text{ cm}^3/\text{g}}{22414 \text{ cm}^3/\text{mol}} \times 6.023 \times 10^{23} \frac{\text{molecules}}{\text{mol}}$$

$$= 16.05 \times 10^{18} \text{ molecules/g}$$

Active metal surface area (per gram of metal)

$$MSA_s = S_f \times \frac{V_{ads}}{V_g} \times \frac{100\%}{\%M} \times N_A \times \sigma_m \times \frac{m^2}{10^{18} \text{ nm}^2}$$

S_f	=	stoichiometry factor, CO on Pd	1
V_{ads}	=	volume adsorbed	0.5976 cm ³ /g
V_g	=	molar volume of gas at STP	22414 cm ³ /mol
%M	=	weight percent of the active metal	0.8 %
N_A	=	Avogadro's number	6.023 × 10 ²³ molecules/mol
σ_m	=	cross-sectional area of active metal atom	0.0787 nm ²

$$MSA_s = 1 \times \frac{0.5976 \text{ cm}^3/\text{g}}{22414 \text{ cm}^3/\text{mol}} \times \frac{100\%}{0.8\%} \times 6.023 \times 10^{23} \frac{\text{molecules}}{\text{mol}} \times 0.0787 \text{ nm}^2$$

$$\times \frac{m^2}{10^{18} \text{ nm}^2}$$

$$= 157.90 \text{ m}^2/\text{g}_{\text{metal}}$$

Average crystallite size

$$d = \frac{F_g}{\rho \times MSA_m} \times \frac{m^3}{10^6 cm^3} \times \frac{10^9 nm}{m}$$

F_g	=	crystallite geometry factor (hemisphere = 6)	6
ρ	=	specific gravity of the active metal	12.0 g/cm ³
MSA_m	=	active metal surface area per gram of metal	157.90 m ² /g _{metal}

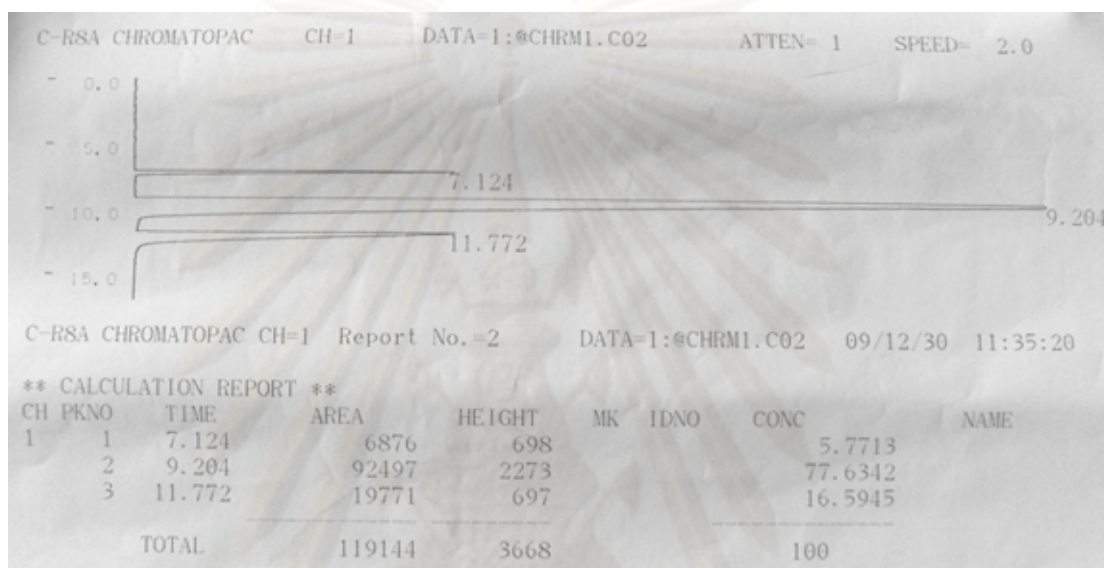
$$d = \frac{6}{12g/cm^3 \times 31.68m^2/g} \times \frac{m^3}{10^6 cm^3} \times \frac{10^9 nm}{m} = 3.17nm$$



ศูนย์วิทยทรัพยากร
จุฬาลงกรณ์มหาวิทยาลัย

APPENDIX C

CHROMATOGRAMS FROM GAS CHROMATOGRAPHY



Peak no.	Time	Name
1	7.124	Ethylbenzene
2	9.204	Styrene
3	11.772	Phenylacetylene

ศูนย์วิทยาศาสตร์
จุฬาลงกรณ์มหาวิทยาลัย

APPENDIX D

CALCULATION OF PHENYLACTYLENE CONVERSION
AND STYRENE SELECTIVITY

The catalytic performance for the phenylacetylene (PA) hydrogenation was evaluated in terms of activity for phenylacetylene conversion and styrene selectivity.

Activity of the catalyst performed in term of phenylacetylene conversion. Phenylacetylene conversion is defined as moles of phenylacetylene converted with respect to phenylacetylene in feed:

$$\text{PA conversion (\%)} = \frac{\text{Mole of PA in feed} - \text{mole of PA in product}}{\text{Mole of PA in feed}} \times 100$$

Selectivity of product is defined as mole of styrene (ST) formed with respect to mole of styrene and ethylbenzene was obtained:

$$\text{Selectivity of ST (\%)} = \frac{\text{Mole of ST formed}}{\text{Mole of total product}} \times 100$$

ศูนย์วิทยทรัพยากร
จุฬาลงกรณ์มหาวิทยาลัย

APPENDIX E

CALCULATION OF TURNOVER OF FREQUENCY

$$\begin{aligned} \text{TOF} &= \frac{\text{rate}}{\text{number of active site}} \\ &= \frac{\text{molecule substrate converted}}{\text{g cat} \times \text{min}} \times \frac{\text{g cat}}{\text{active site}} \times \frac{\text{min}}{\text{s}} \end{aligned}$$

While, metal active site = molecule/ g catalysts

Then,

$$\text{TOF} = [\text{s}^{-1}]$$

ศูนย์วิทยทรัพยากร
จุฬาลงกรณ์มหาวิทยาลัย

VITA

Miss Napaporn Tiengchad was born in April 5th, 1985 in Rayong, Thailand. She finished high school from Huay-yang sukka School, Rayong in 2003. After that, she studied at Burapha University, Chonburi, Thailand for 4 years and received Bachelor's Degree from the department of Chemical Engineering in June 2007. Then, she required to study in the Master's Degree and received scholarship from the department of chemical engineering, Chulalongkorn University in 2008.

In October 2009, she participated in the 19th Thailand Chemical Engineering and Applied Chemistry Conference, Kanjanaburi, Thailand for oral presentation and published for "Palladium nanoparticles supported on various mesoporous silica prepared from colloidal palladium".



ศูนย์วิทยทรัพยากร
จุฬาลงกรณ์มหาวิทยาลัย